Measurements of the CP structure of Higgs-boson couplings with the ATLAS experiment

Simen Hellesund
On Behalf of the ATLAS Collaboration

University of Bergen

DIS2024
Grenoble – 09.04.24

Searches for CP violation in Bosonic Higgs Interactions

Bosonic Higgs Vertex - HVV

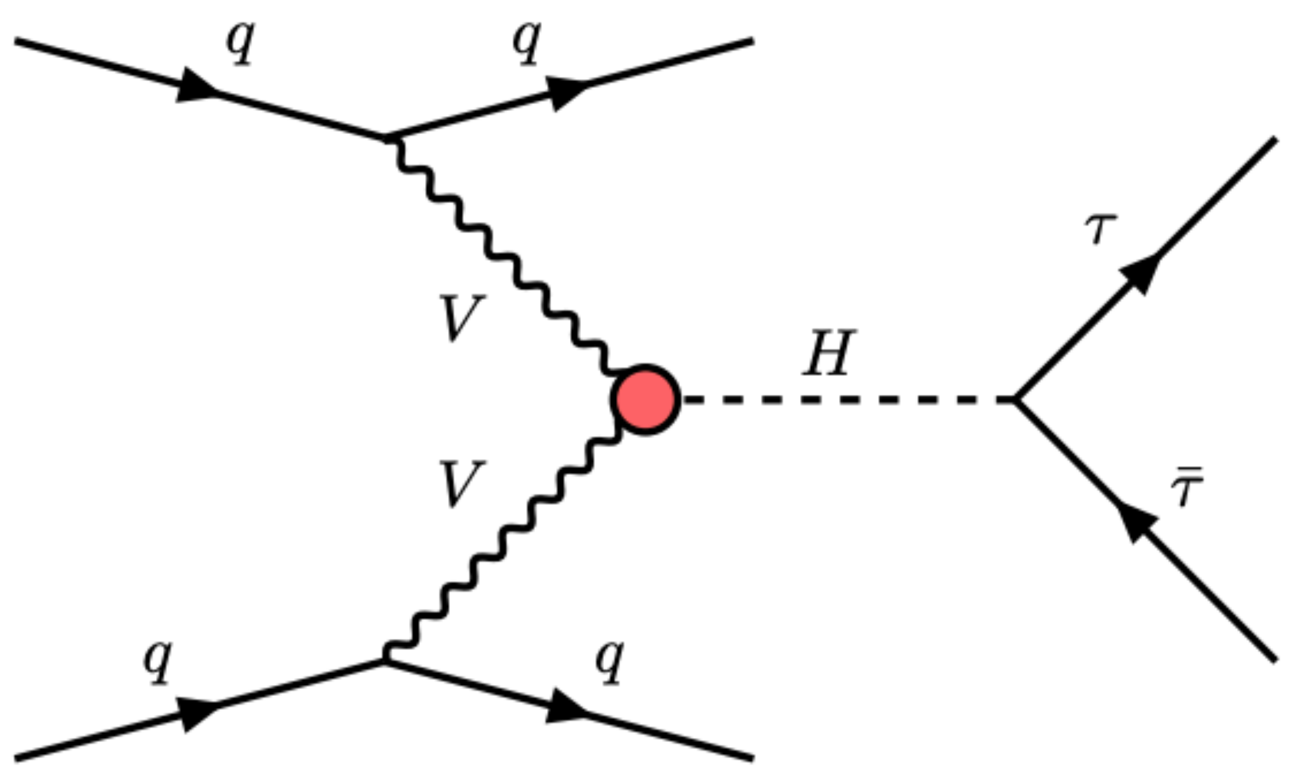

VBF H → $\tau\bar{\tau}$

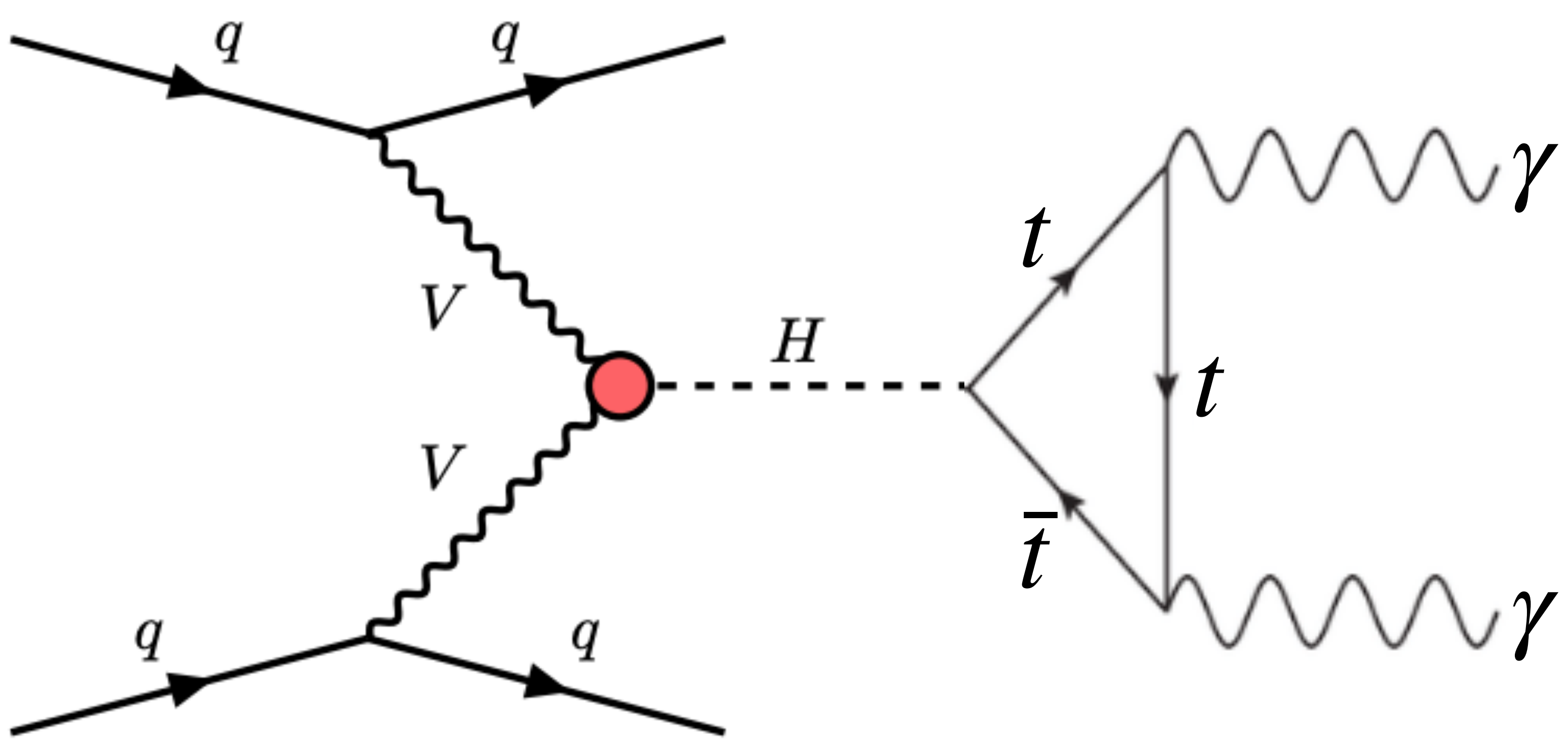

VBF H → $\gamma\gamma$

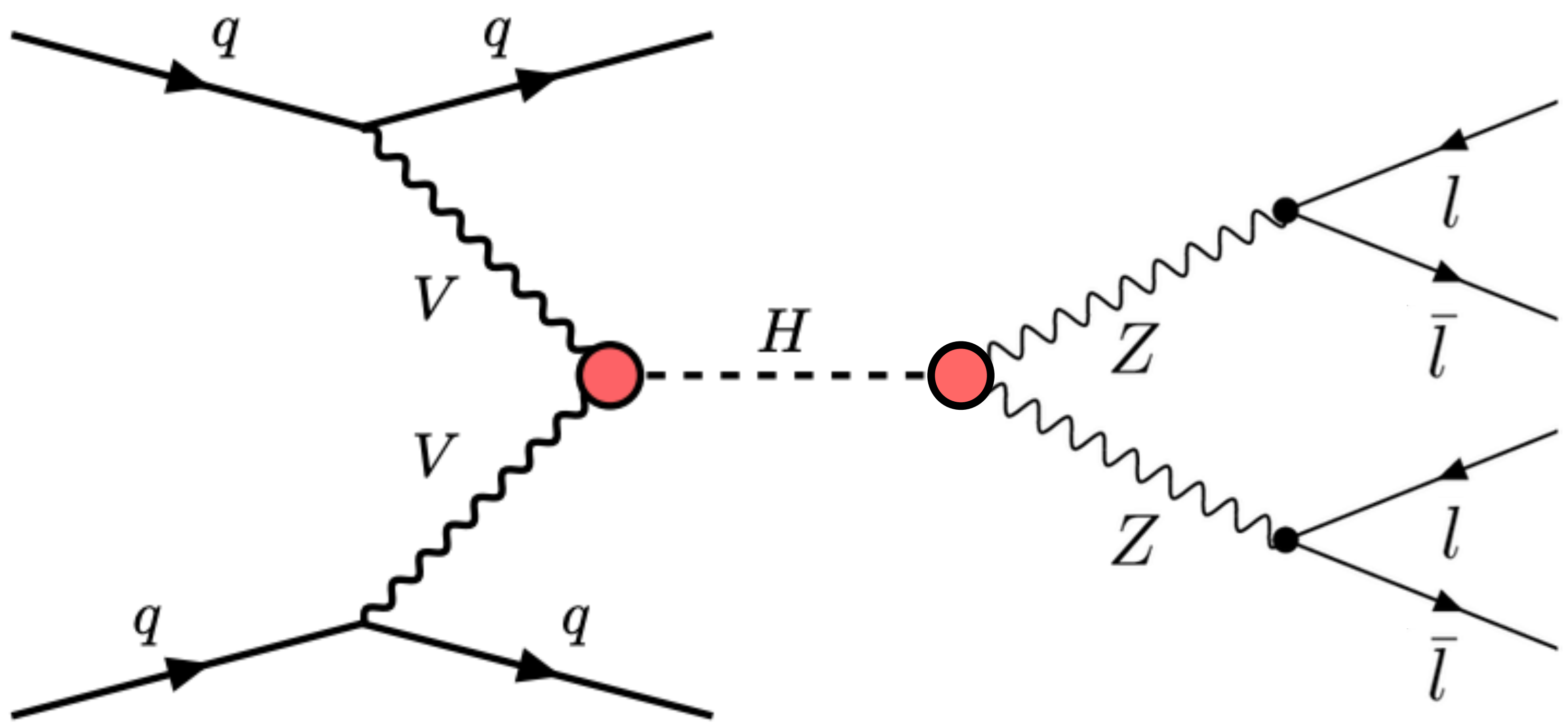

H → $ZZ^* \rightarrow 4l$

- SMEFT squared matrix element:

$$|\mathcal{M}|^2 = |\mathcal{M}_{SM}|^2 + 2\sum_i \frac{c_i}{\Lambda^2} Re(\mathcal{M}^*_{SM}\mathcal{M}_{BSM,i}) + \sum_i \sum_j \frac{c_i c_j}{\Lambda^4} Re(\mathcal{M}^*_{BSM,j}\mathcal{M}_{BSM,i})$$

H → ZZ* → 4l

arXiv:2304.09612 (submitted to JHEP)

- Search for CP violation in the HVV vertex in both VBF Higgs production and in Higgs decays to four leptons.
- *Optimal Observable* (OO) used as discriminant, calculated from matrix elements.
- In the SM, OO distribution is symmetric around zero. Asymmetric for CP-odd signals.
- Set limits on SMEFT couplings in Warsaw, Higgs, and HISZ bases.

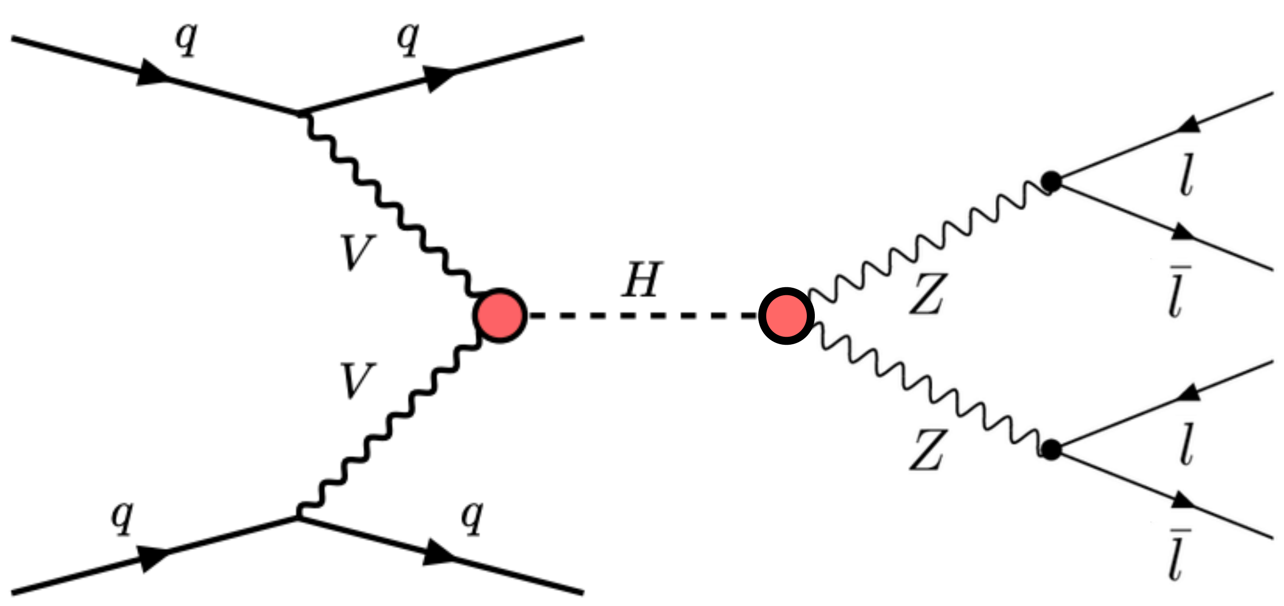

$$OO = \frac{2Re(\mathcal{M}^*_{SM}\mathcal{M}_{BSM})}{|\mathcal{M}_{SM}|^2}$$

H → 4l Decay

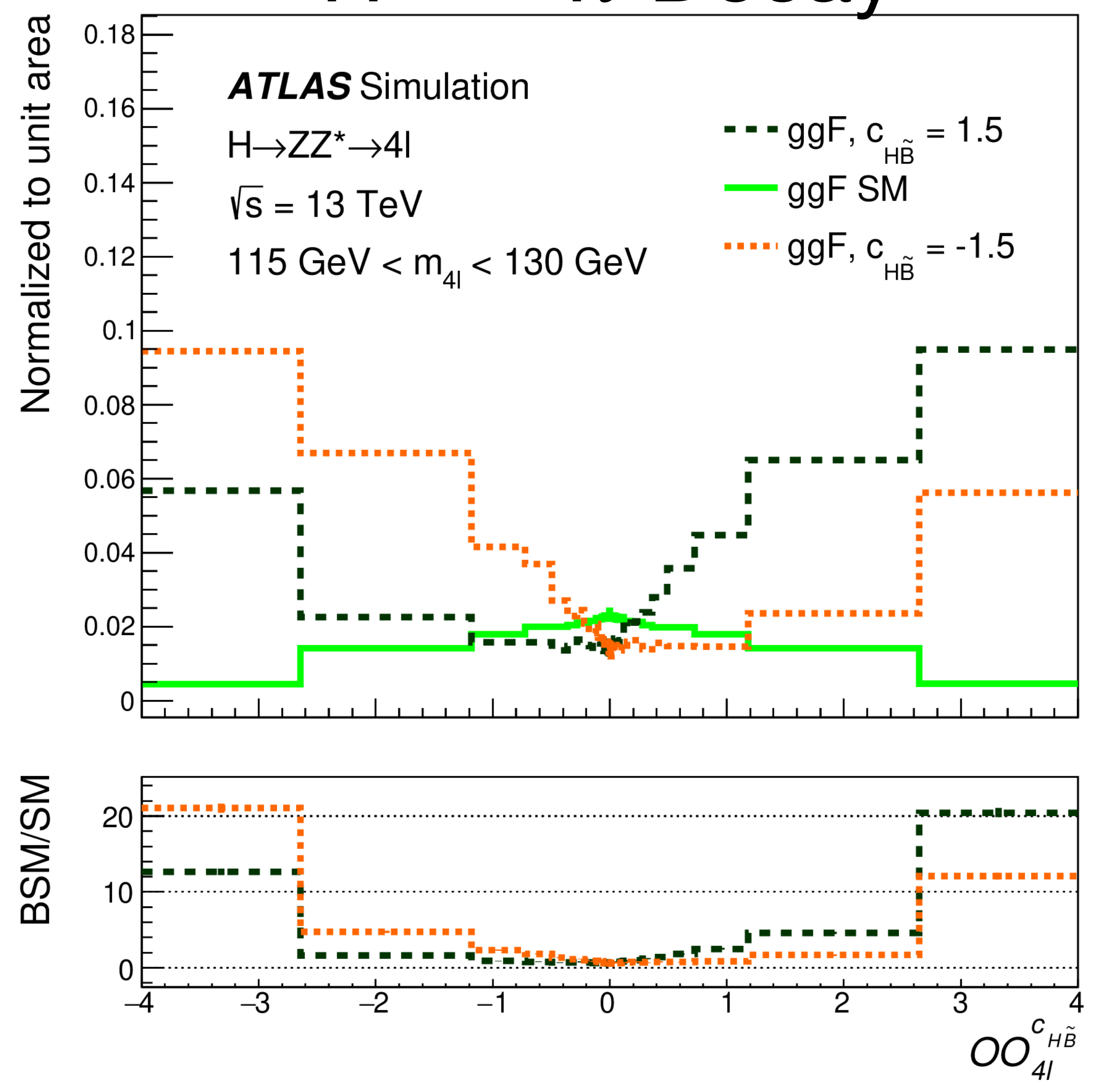

VBF H Production

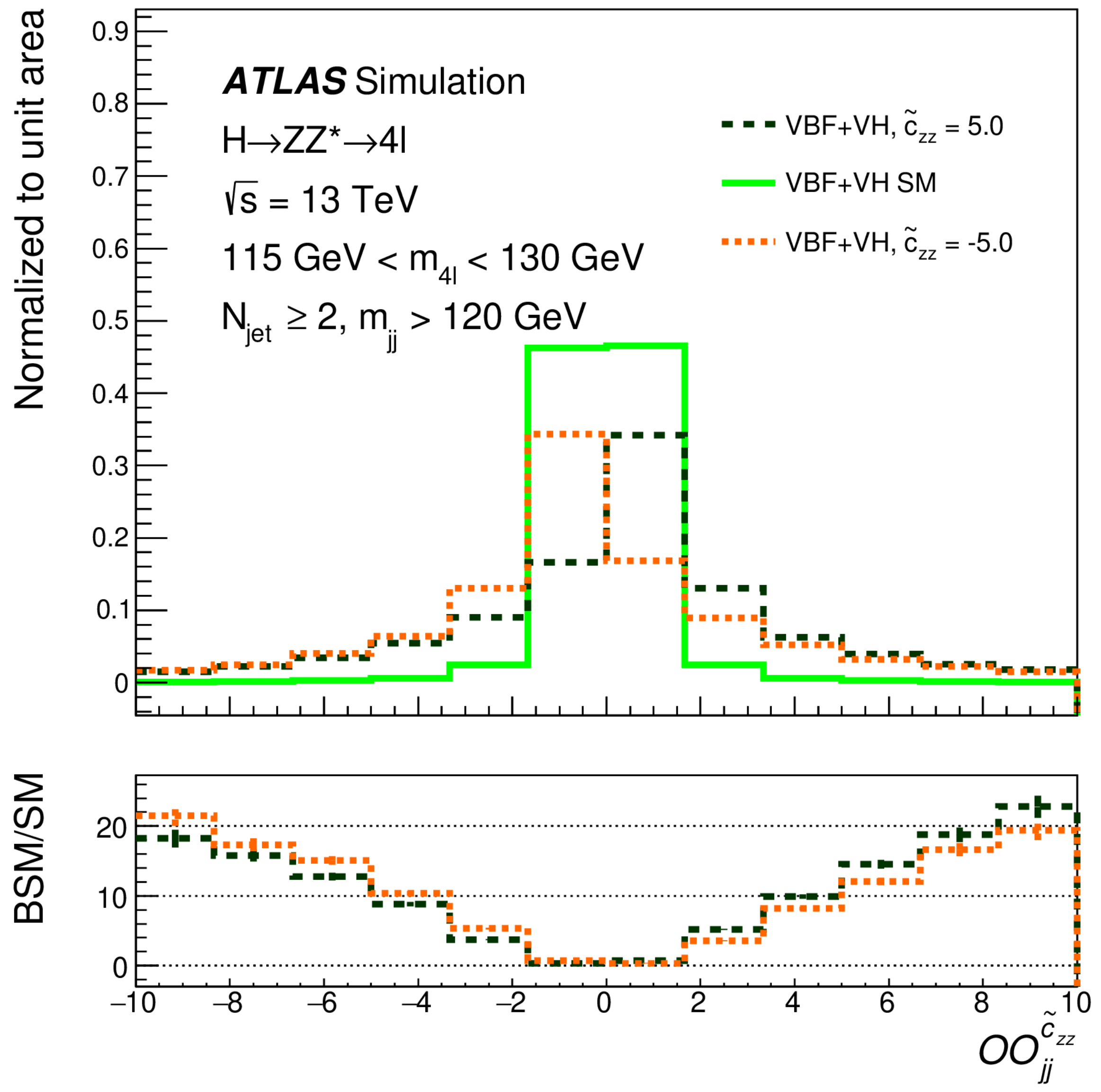

H → ZZ* → 4l

arXiv:2304.09612 (submitted to JHEP)

- ZZ* background normalisation fitted in a mass sideband control region.
- VBF-depleted ggH signal region, and four VBF signal regions defined by the output of a neural net classifier.
- Decay-level fit in VBF-depleted signal region.
- Production level fit in VBF signal regions.
- Shape only, signal normalisation is floating in the fit.

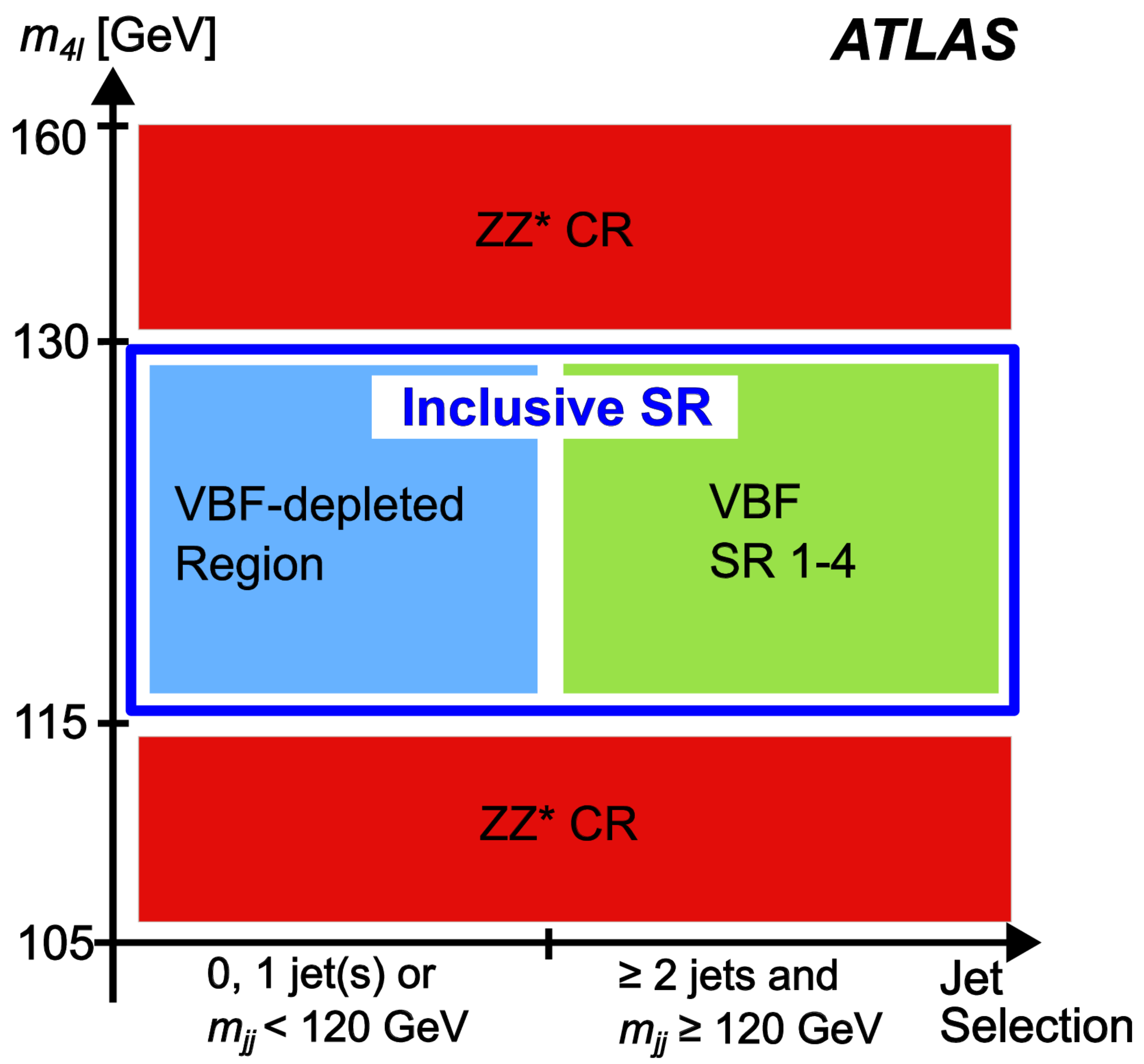

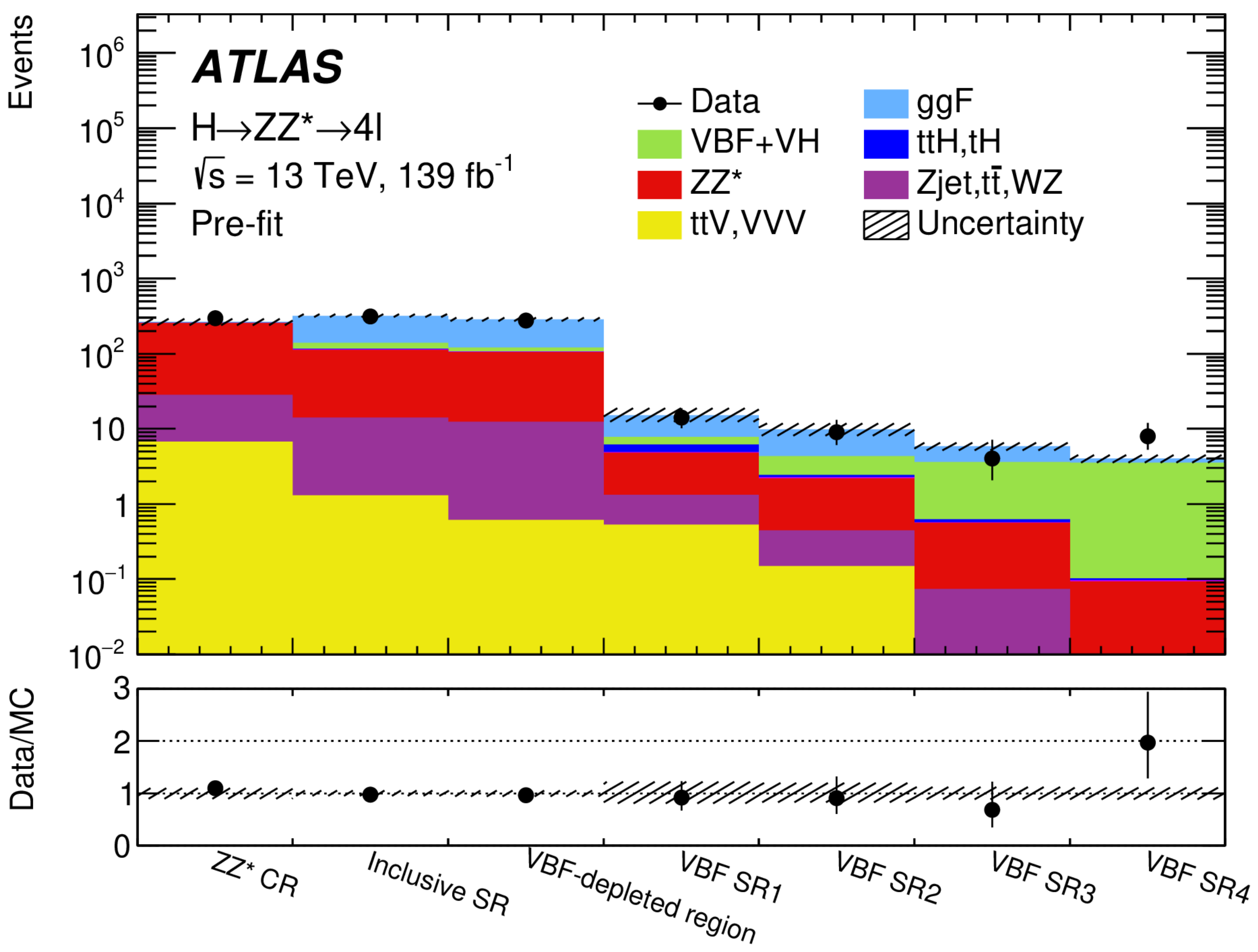

$H \rightarrow ZZ^* \rightarrow 4l$

arXiv:2304.09612 (submitted to JHEP)

Higgs Basis

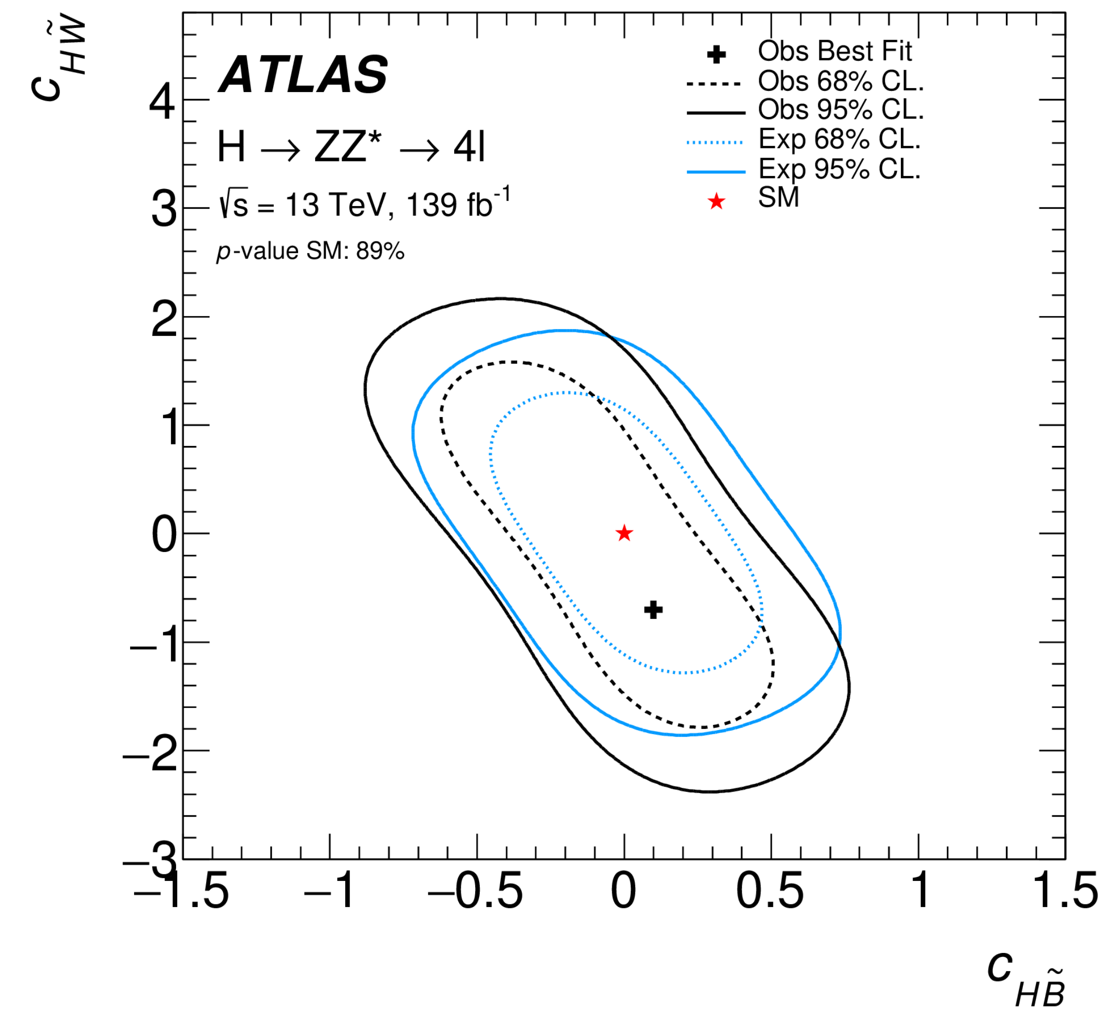

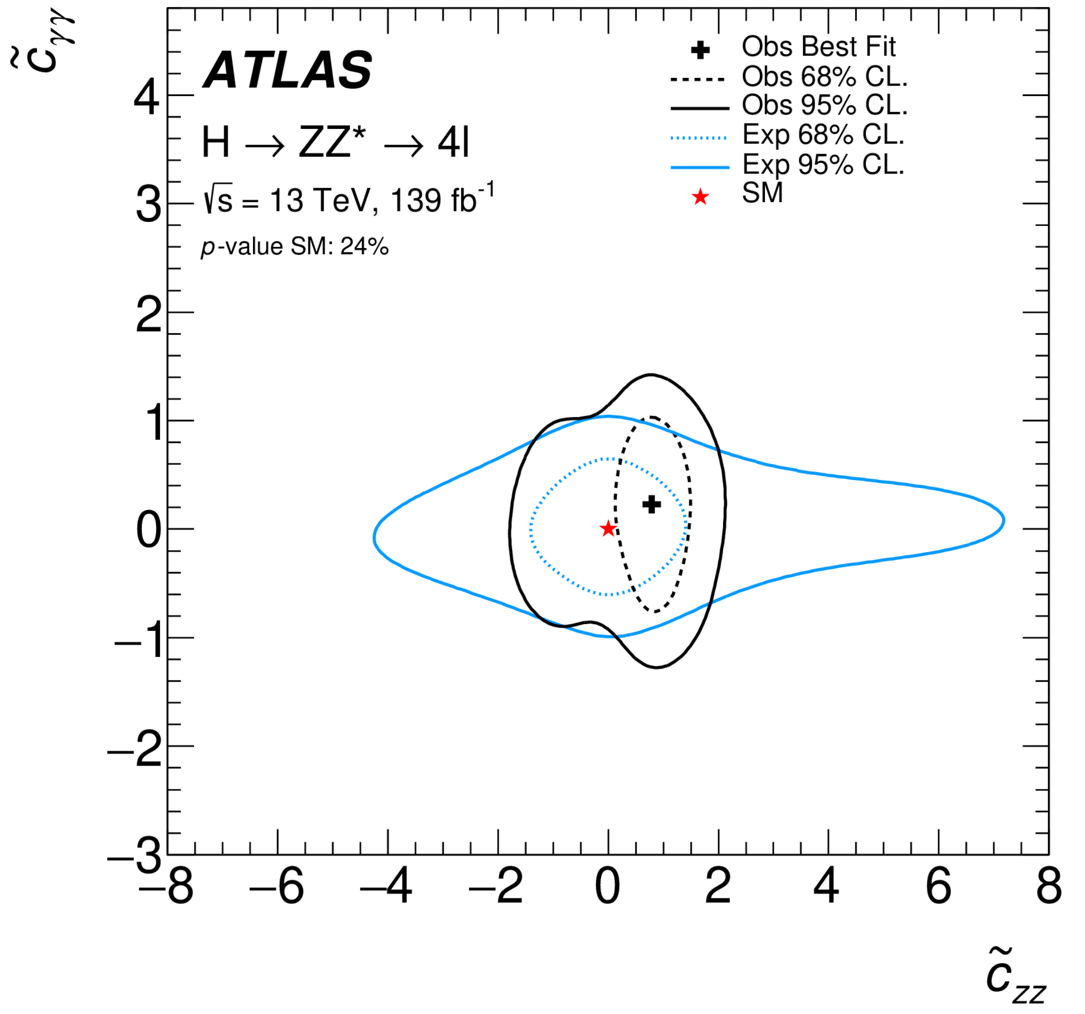

Warsaw Basis

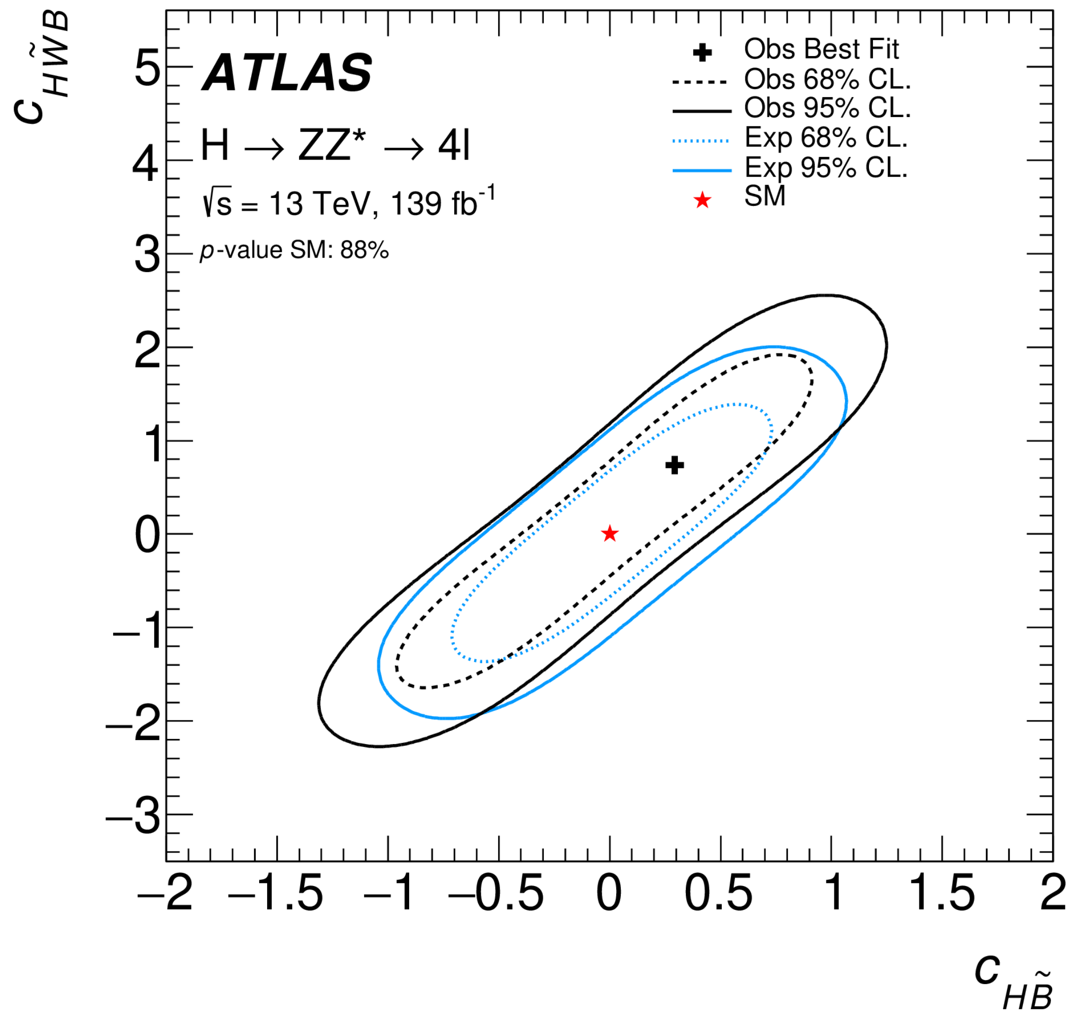

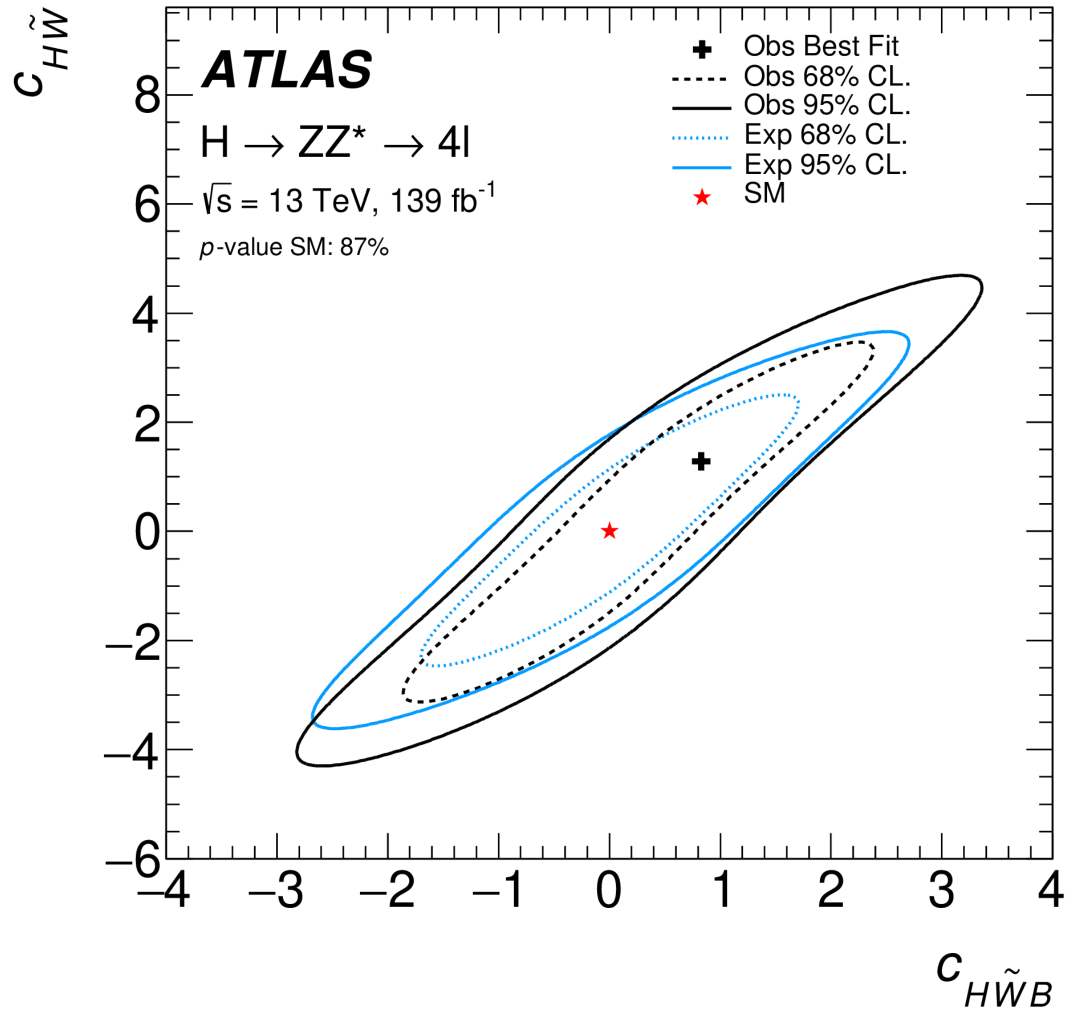

SMEFT Coefficients

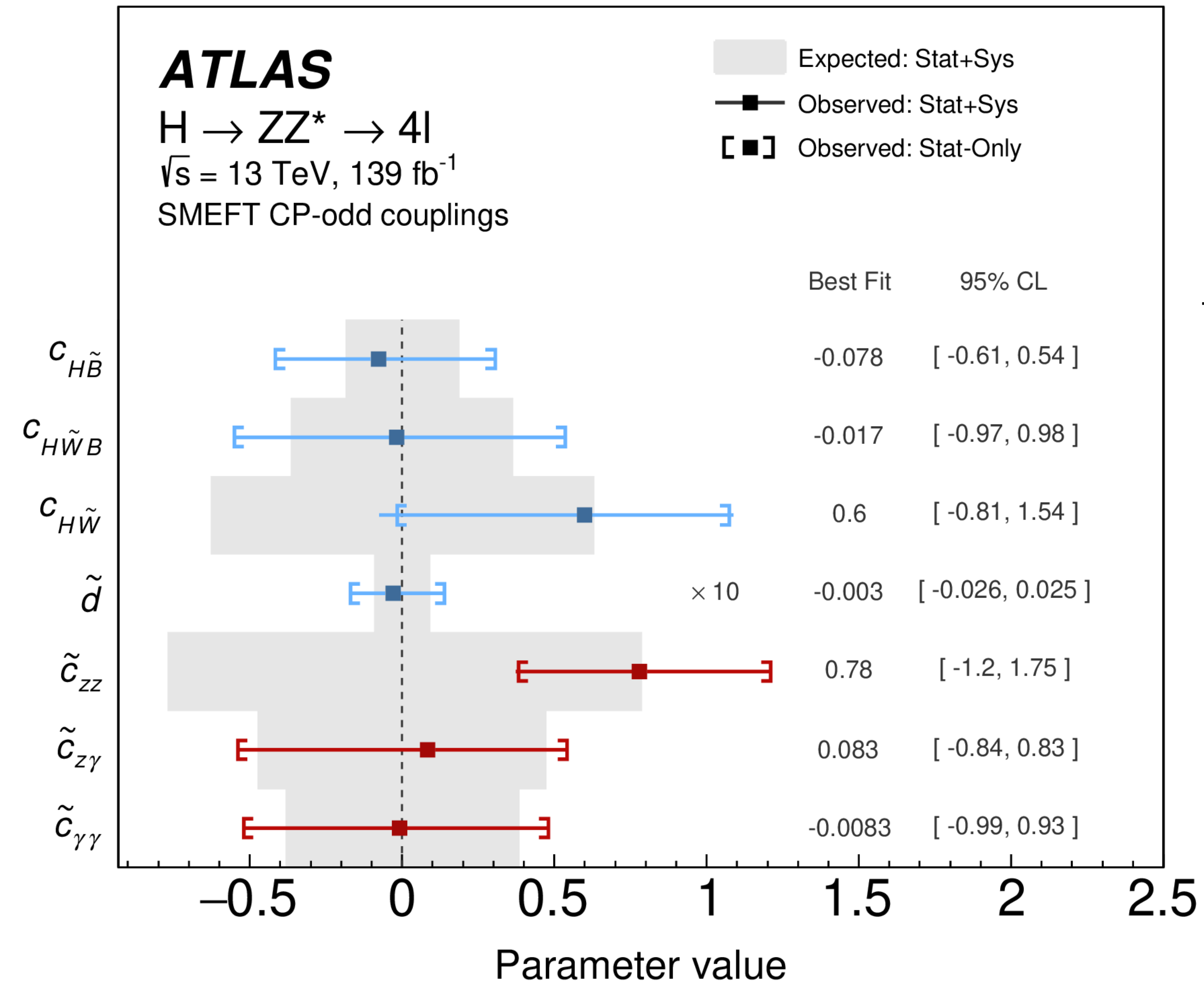

Fit Type
Decay
Decay
Combined
Decay
Production
Decay
Decay

- In agreement with the SM.
- Limits are dominated by the interference matrix element term.
  - Implies low expected sensitivity to dimension eight operators.

VBF H → $\gamma\gamma$

[Phys. Rev. Lett. 131 (2023) 061802](https://doi.org/10.1103/PhysRevLett.131.061802)

- Search for CP violation in Higgs VBF production, with the Higgs decaying to a photon pair.
- Search performed in the Warsaw ($c_{H\widetilde{W}}$) and HISZ ($\tilde{d}$) bases.
- Two boosted decision tree (BDT) classifiers are used: one to separate VBF signal from ggH contamination and one to separate VBF events from continuum $\gamma\gamma$ background events.
- Three signal regions are defined based on cuts in the classifier outputs: TT, TL, and LT

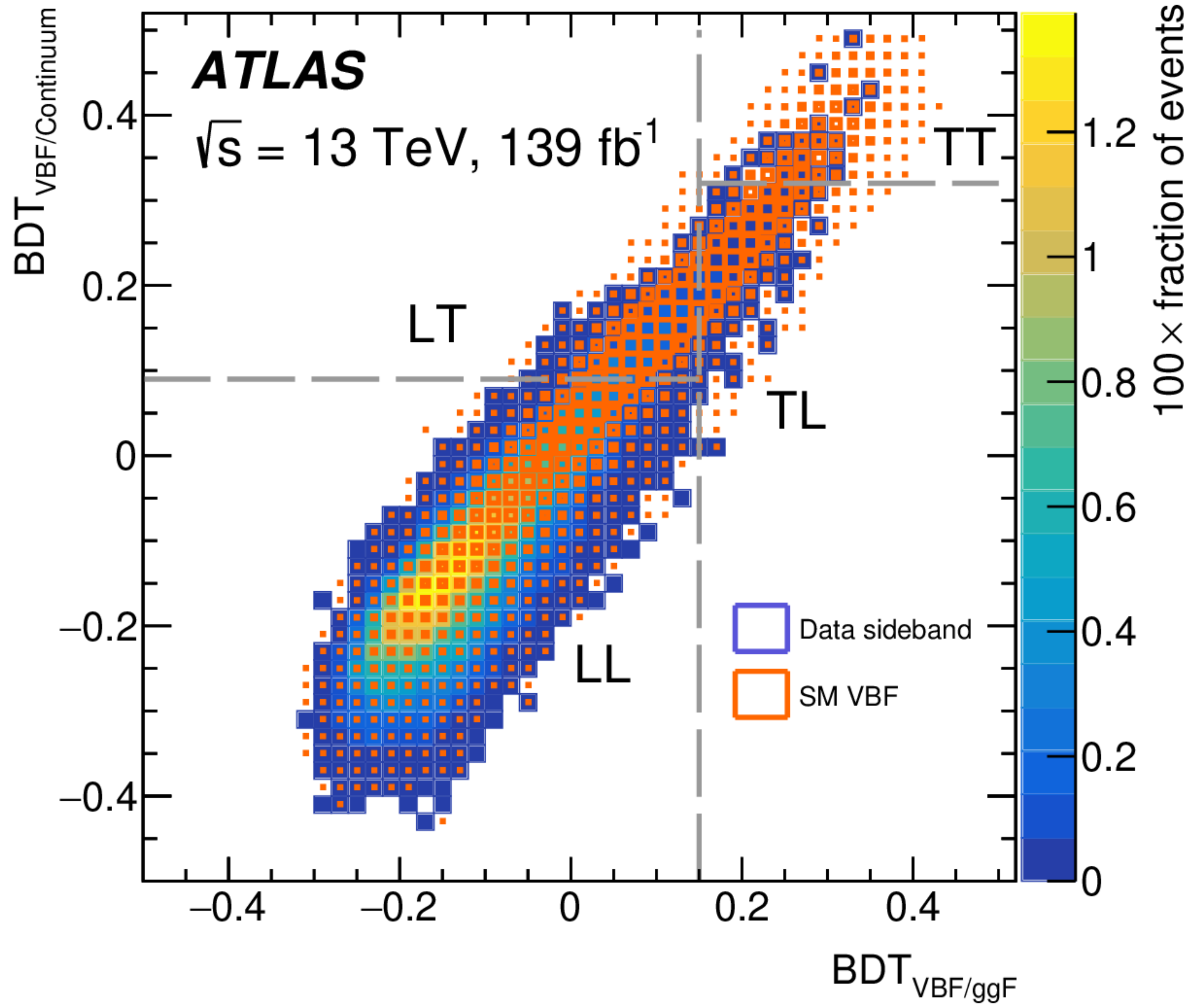

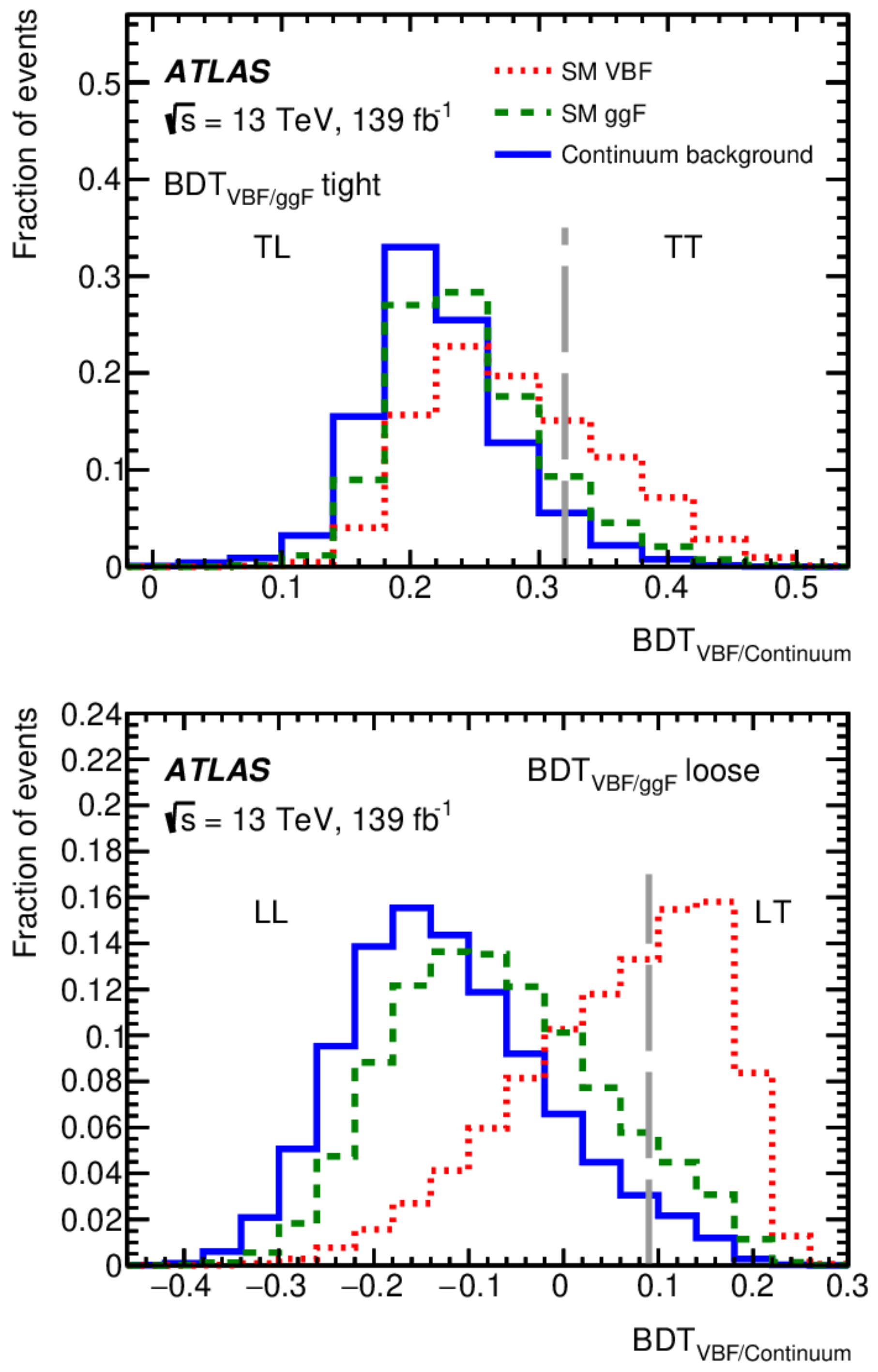

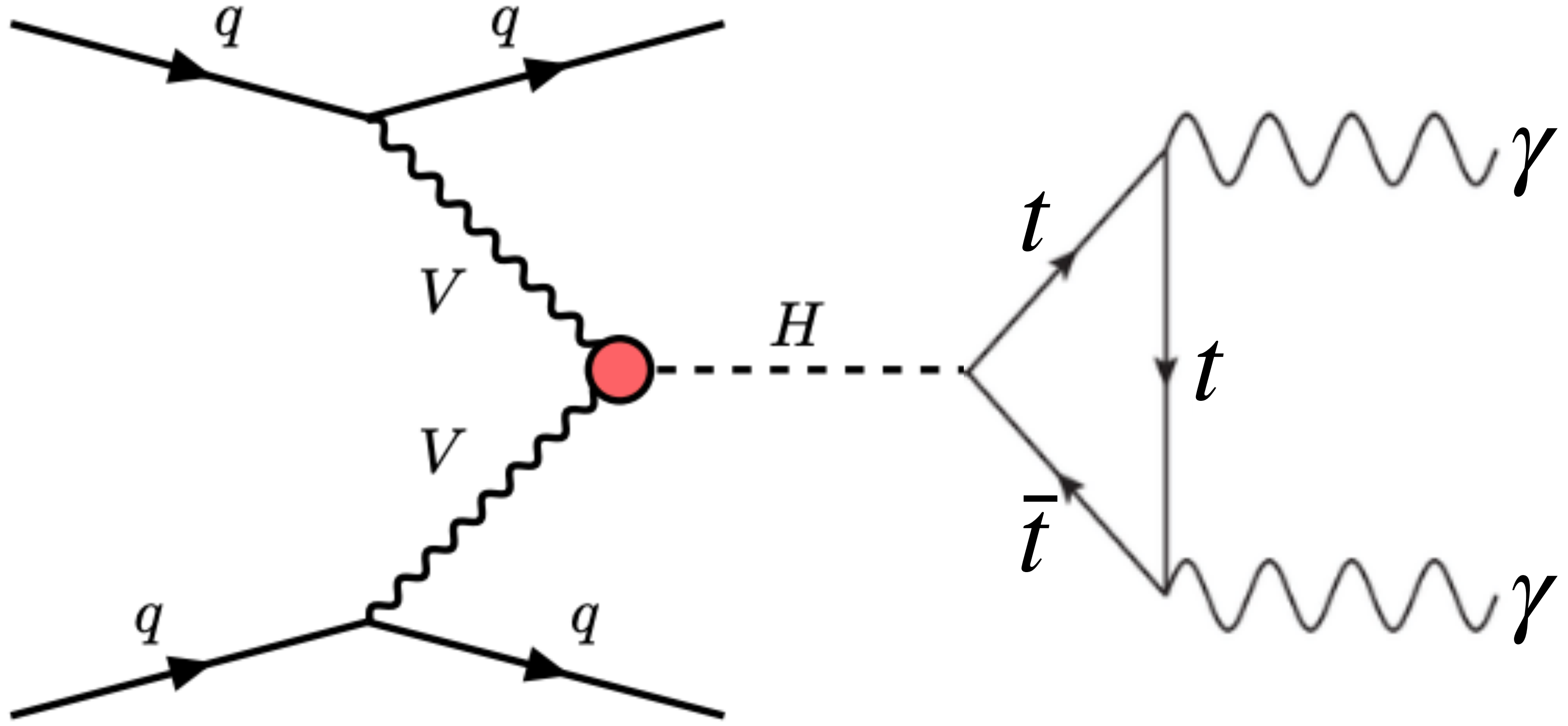

VBF H $\rightarrow \gamma\gamma$

- Perform an unbinned fit to $m_{\gamma\gamma}$ in each signal region, and in each bin of the optimal observable distribution.
- Signal and background shapes are modelled by analytic functions.
- Normalisation of the signal floats in the fit, only considering the OO shape.

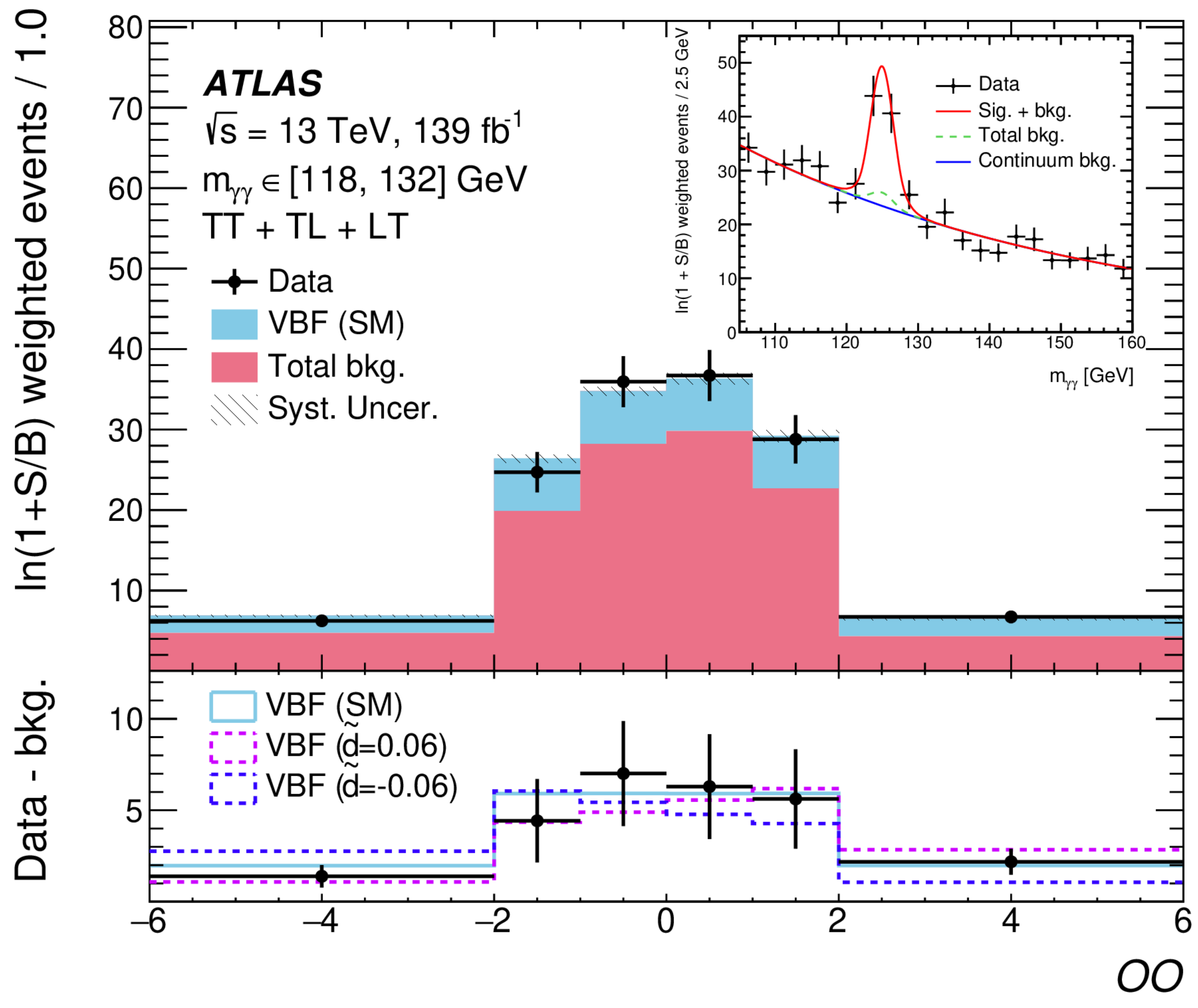

VBF H $\rightarrow \gamma\gamma$

Phys. Rev. Lett. 131 (2023) 061802

- Confidence intervals at 95%: $\tilde{d}$: $[-0.034, 0.071]$, $c_{H\tilde{W}}$: $[-0.55, 1.07]$
- Consistent with the SM.
- Again, the CP-odd interference term is dominant, as expected for a shape analysis.
- The 68% $c_{H\tilde{W}}$ confidence limit is about twice as restrictive as in the previously shown 4l analysis.
- Combine $\tilde{d}$ result with VBF H $\rightarrow \tau\bar{\tau}$ analysis using a partial (36.1 fb^{-1}) Run 2 dataset for a confidence interval at 95% of $\tilde{d}$: $[-0.034, 0.057]$
  - Full Run 2 VBF H $\rightarrow \tau\bar{\tau}$ analysis is under way.

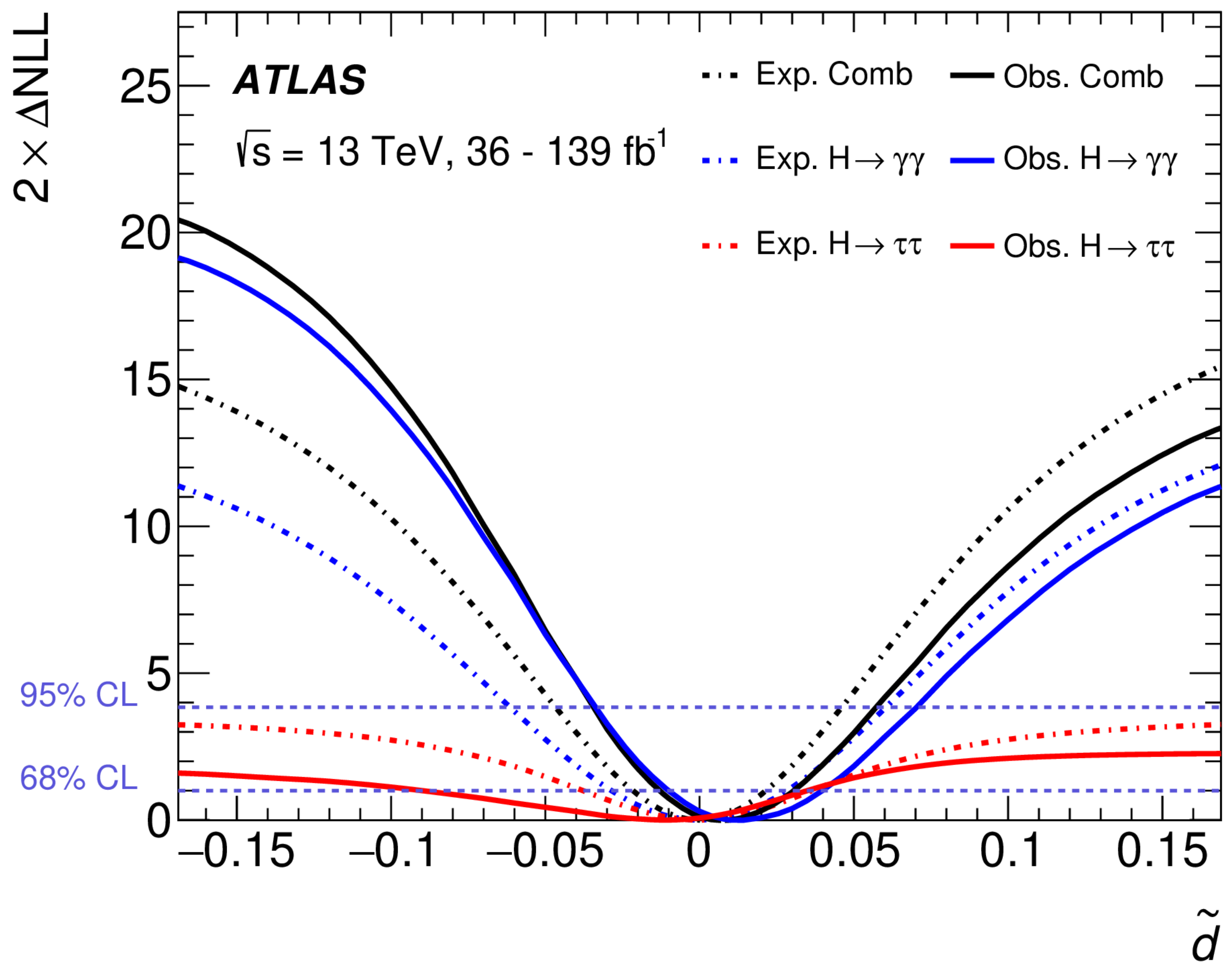

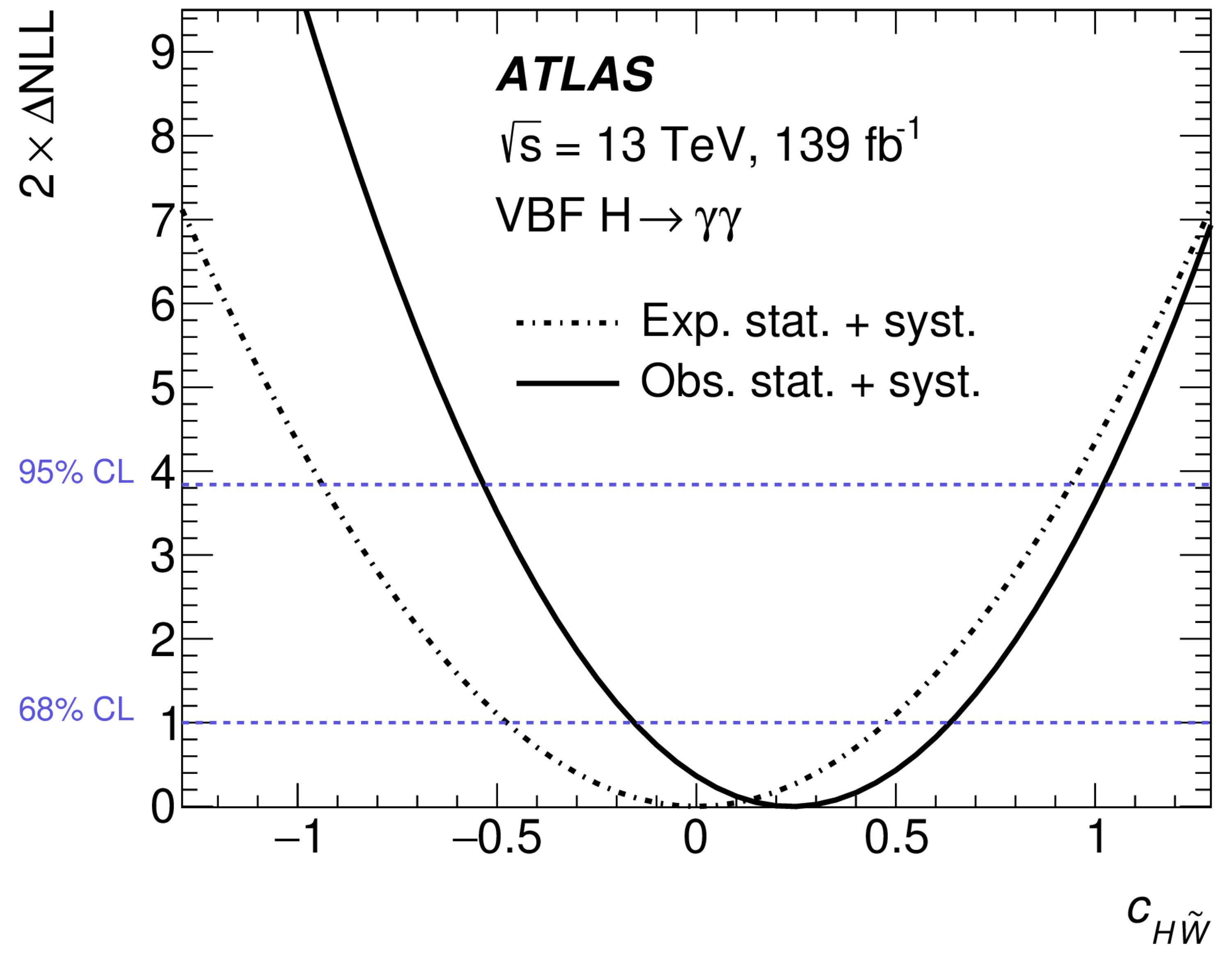

	68% (obs.)	95% (obs.)
$\tilde{d}$ (inter. only)	[−0.011, 0.036]	[−0.032, 0.059]
$\tilde{d}$ (inter.+quad.)	[−0.010, 0.040]	[−0.034, 0.071]
$\tilde{d}$ from $H \rightarrow \tau\tau$	[−0.090, 0.035]	-
Combined $\tilde{d}$	[−0.012, 0.030]	[−0.034, 0.057]
$c_{H\tilde{W}}$ (inter. only)	[−0.16, 0.64]	[−0.53, 1.02]
$c_{H\tilde{W}}$ (inter.+quad.)	[−0.15, 0.67]	[−0.55, 1.07]

Searches for CP violation in Fermionic Higgs Interactions

Fermionic Higgs Vertices - Yukawa

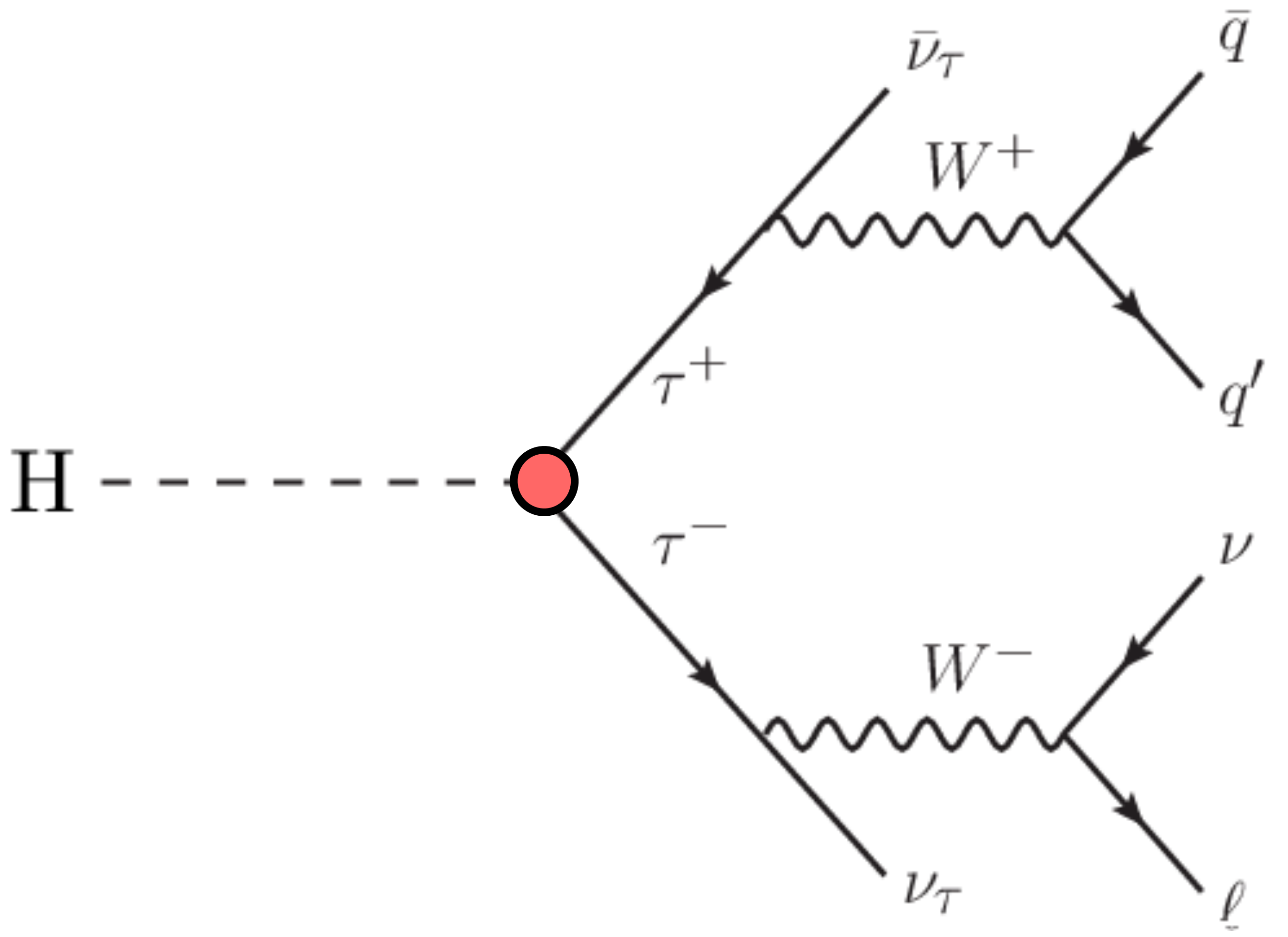

H$\tau\bar{\tau}$ Vertex

- In fermionic interactions, CP-odd contribution may contribute at tree level.
- CP-odd contribution determined by the CP-mixing angle α and the coupling strength parameter κ'.

$$\mathscr{L}_{t\bar{t}H} = -\kappa_t' y_t \phi \bar{\psi}_t (\cos\alpha + i\gamma_5 \sin\alpha)\psi_t$$

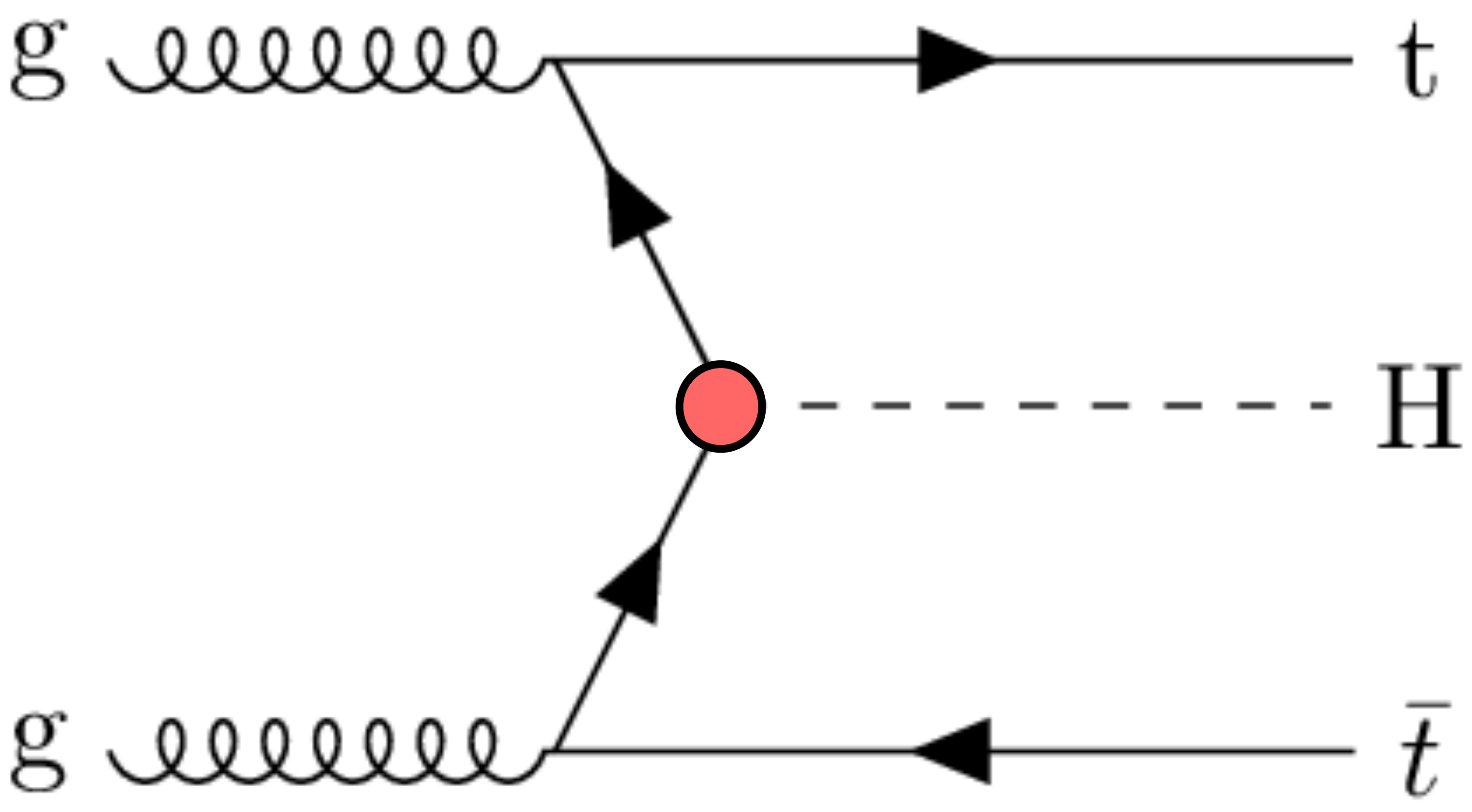

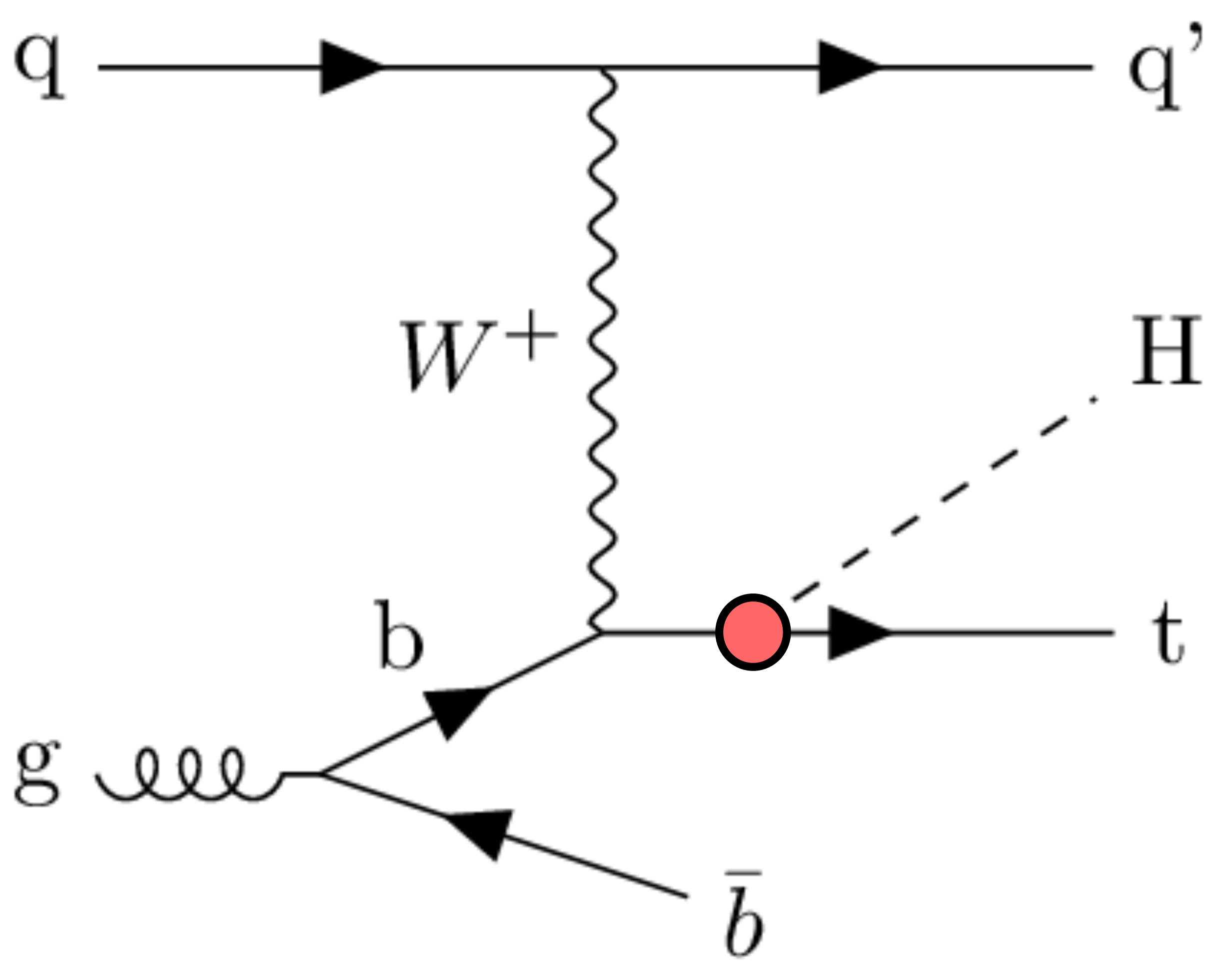

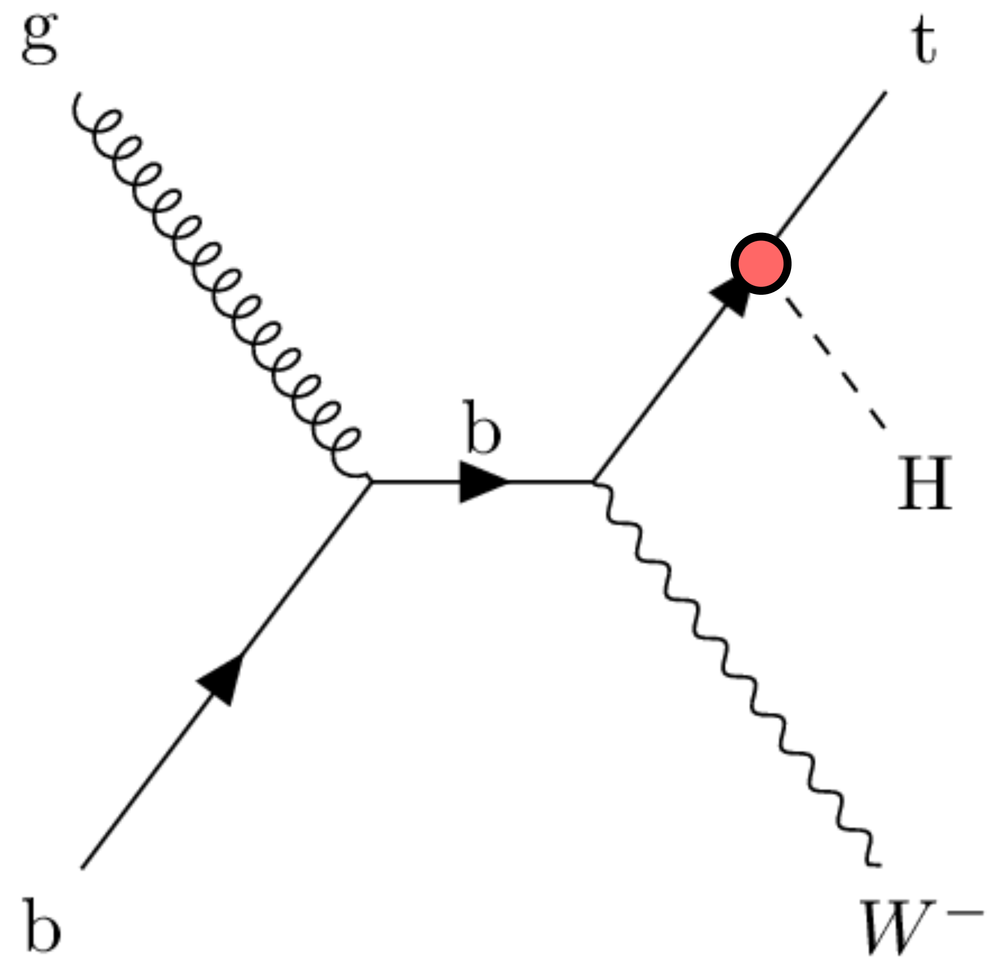

Ht$\bar{\text{t}}$ Vertex

Ht, $Ht\bar{t}$ with $H \to b\bar{b}$

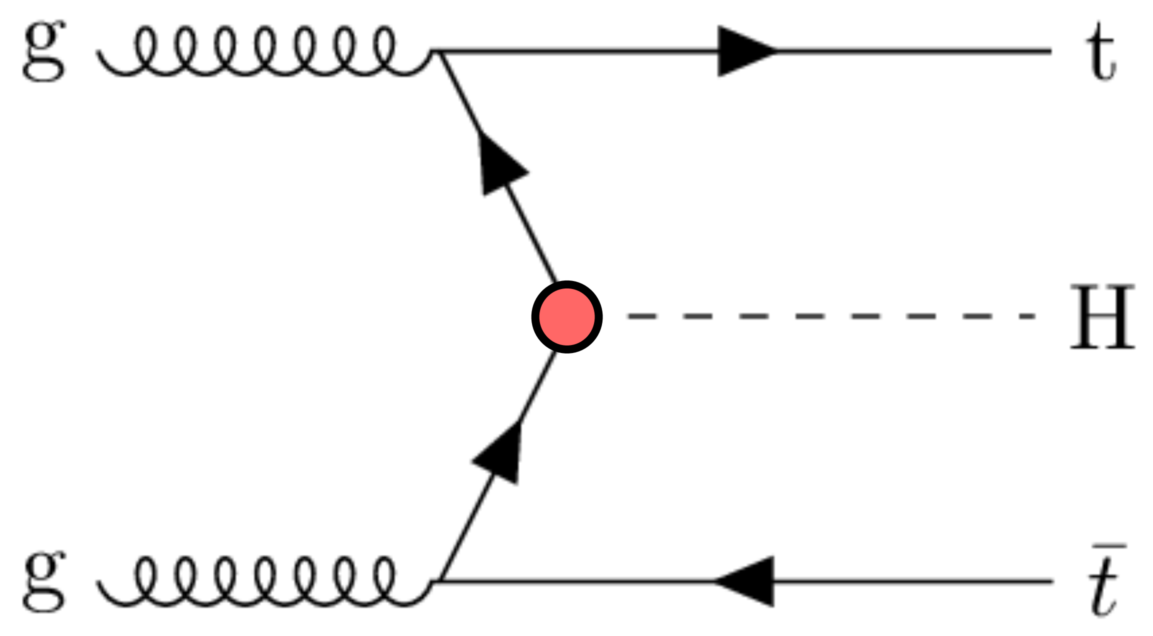

- Analysis targeting $Ht\bar{t}$ and Ht production, with $H \to b\bar{b}$
- Optimised for $Ht\bar{t}$, but Ht processes are also considered signal.
- Two channels, defined by the top pair decay modes:
  - Dileptonic: four b-tagged jets, two charged leptons.
  - l + jets: six jets (four b-tagged), one charged lepton.
- Four signal regions, defined by the output of two BDTs.
- CP-sensitive observables b_2 and b_4, (or BDT output directly)
- p_1 and p_2 are the momentum three-vectors of the two top quarks.

$$b_2 = \frac{(\vec{p}_1 \times \hat{z}) \cdot (\vec{p}_2 \times \hat{z})}{|\vec{p}_1||\vec{p}_2|}$$

$$b_4 = \frac{(\vec{p}_1 \cdot \hat{z})(\vec{p}_2 \cdot \hat{z})}{|\vec{p}_1||\vec{p}_2|}$$

Ht, Ht$\bar{t}$ with H → b$\bar{b}$

[Phys. Lett. B 849 (2024) 138469]

- Simultaneous profile likelihood fit in all four signal regions.
- κ_t' and α are free parameters in the fit.
- Best fit parameters found to be:
  - $\kappa_t' = 0.84^{+0.30}_{-0.46}$
  - $\alpha = 11^{\circ}{}^{+52^{\circ}}_{-73^{\circ}}$

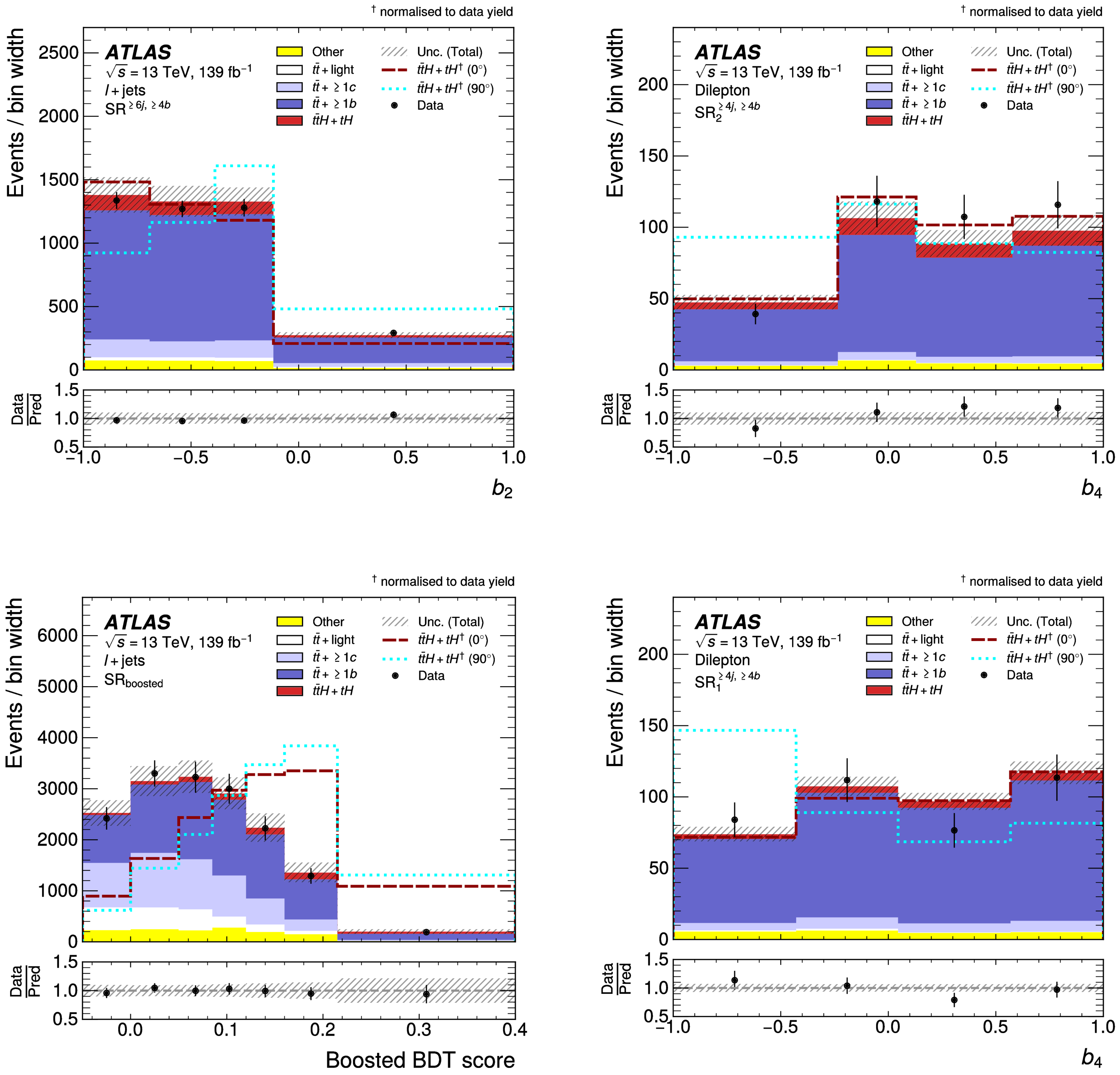

Ht, $Ht\bar{t}$ with $H \rightarrow b\bar{b}$

[Phys. Lett. B 849 (2024) 138469]

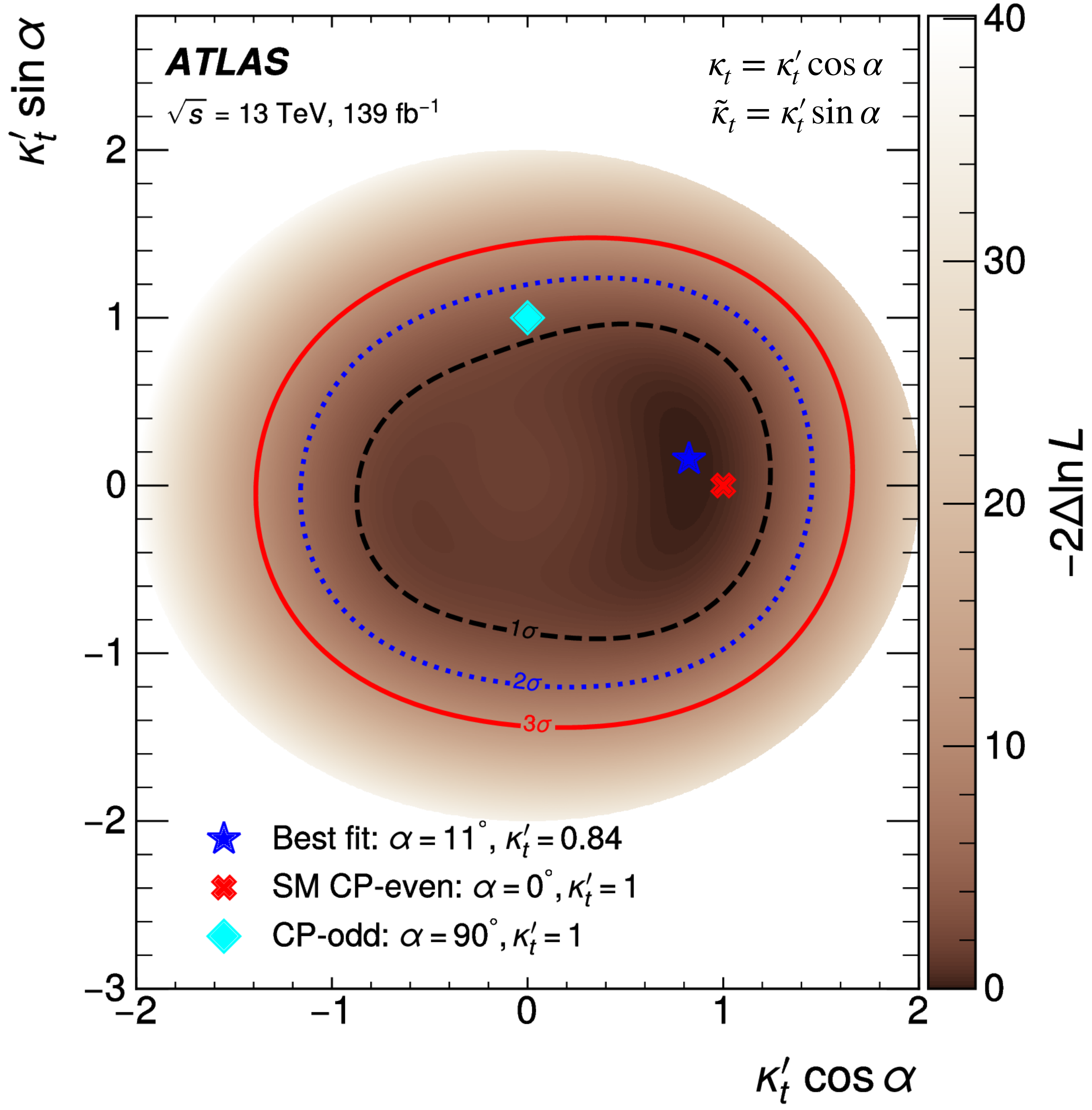

$$\kappa_t' = 0.84^{+0.30}_{-0.46} \qquad \alpha = 11^{\circ}{}^{+52^\circ}_{-73^\circ}$$

- Results are consistent with the SM.
- First probing of the CP properties of the Higgs top Yukawa coupling in this channel.
- The pure CP-odd hypothesis is disfavoured at 1.2 σ.
- The ratio of Ht to $Ht\bar{t}$ cross-sections varies from 0.06 in the SM scenario to more than 1.2 in the pure CP-odd scenario.
  - A dedicated Ht-optimised analysis is underway, focussing on the boosted Higgs region.

H $\rightarrow \tau\bar{\tau}$

Eur. Phys. J. C 83 (2023) 563

- A search for CP violation in Higgs di-tau decays.
- The CP-mixing angle α is encoded in the correlations between the transverse spin components of the tau leptons.
- The signed acoplanarity angle ϕ^*_{CP} between the tau decay planes is sensitive to these spin correlations.
- The analysis targets hadronic and semi-hadronic di-tau decay channels.

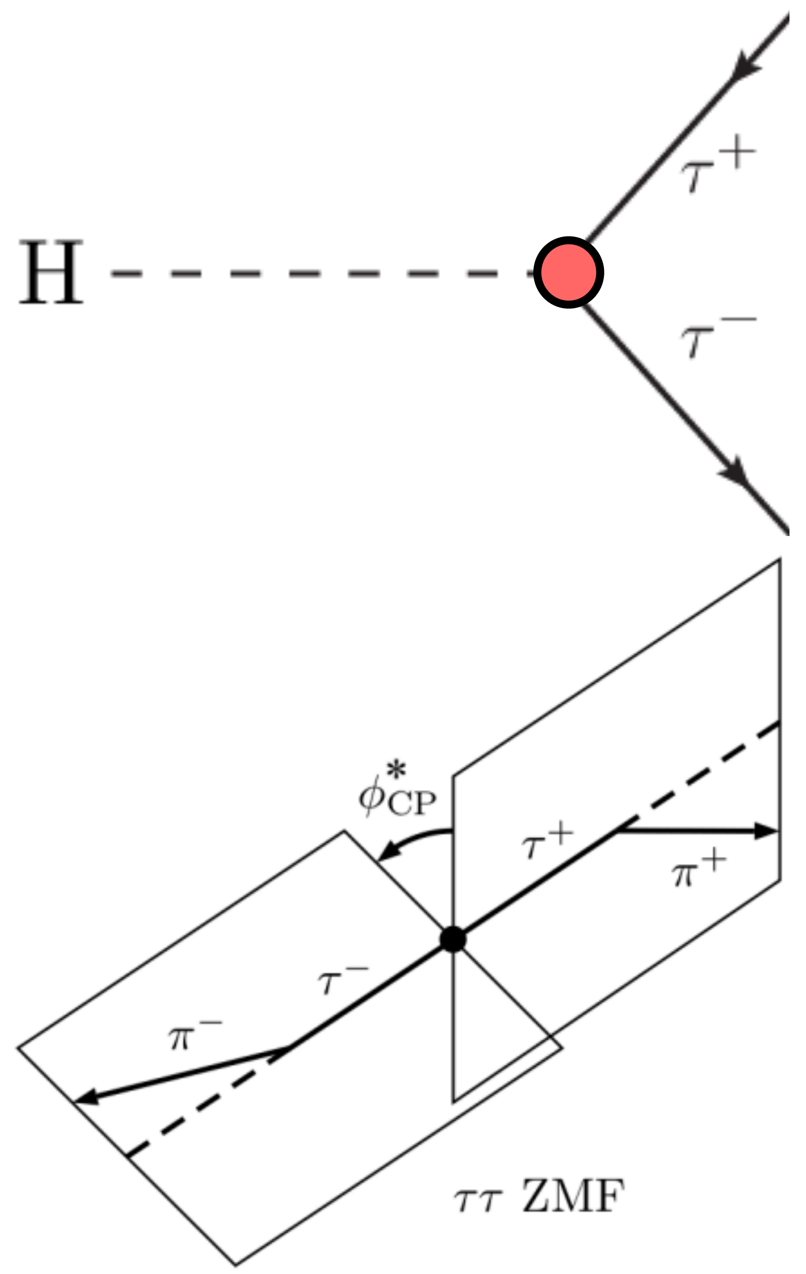

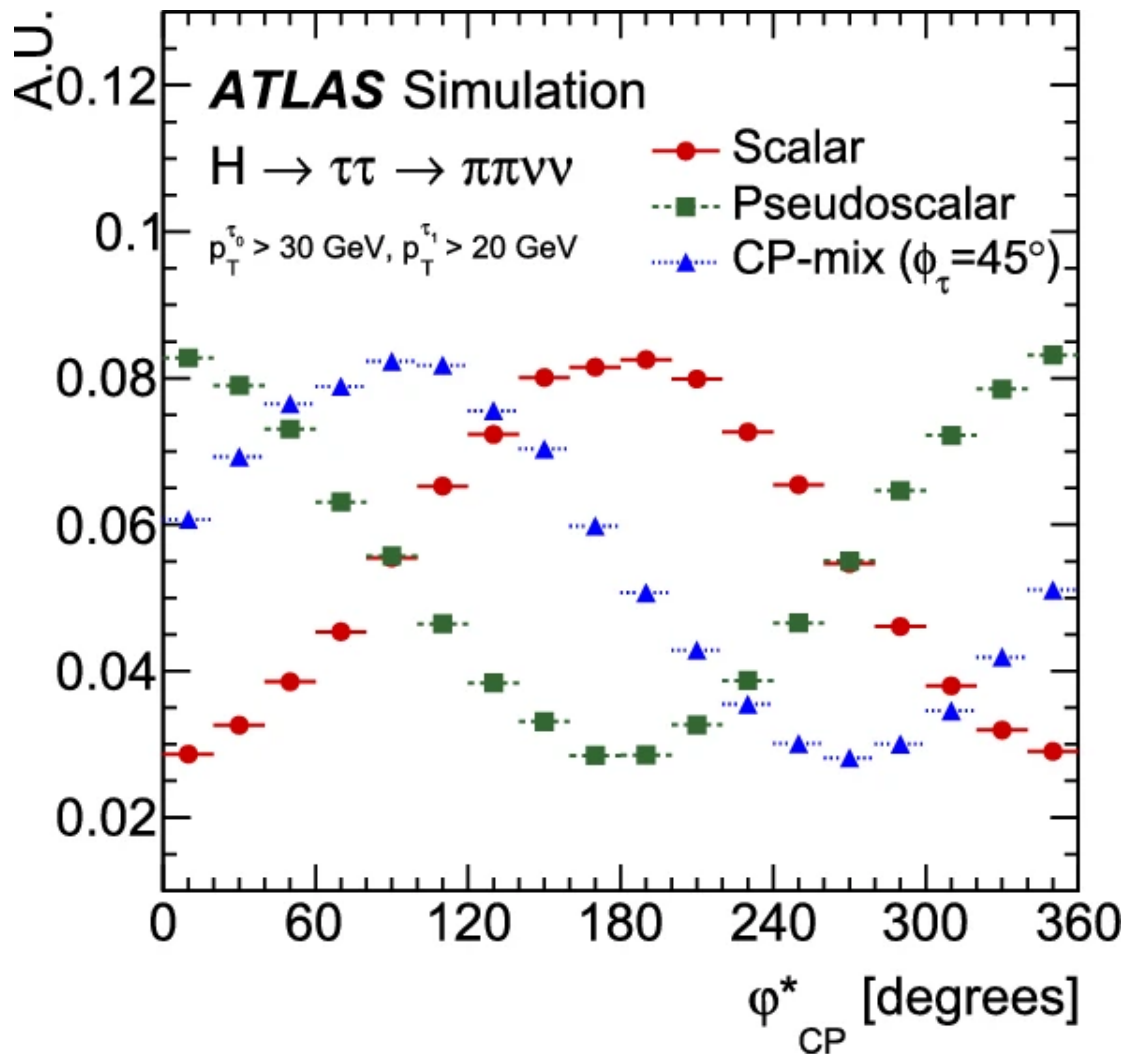

$H \to \tau\bar{\tau}$

Eur. Phys. J. C 83 (2023) 563

- Two VBF (determined by the output of a BDT) and two ggH (boosted) signal regions.
- Further separated into "high", "medium", "low", signal regions, based on tau decay modes, and their sensitivity to tau spin correlations.
- $Z \to \tau\bar{\tau}$ background normalisation determined in a dedicated control region.

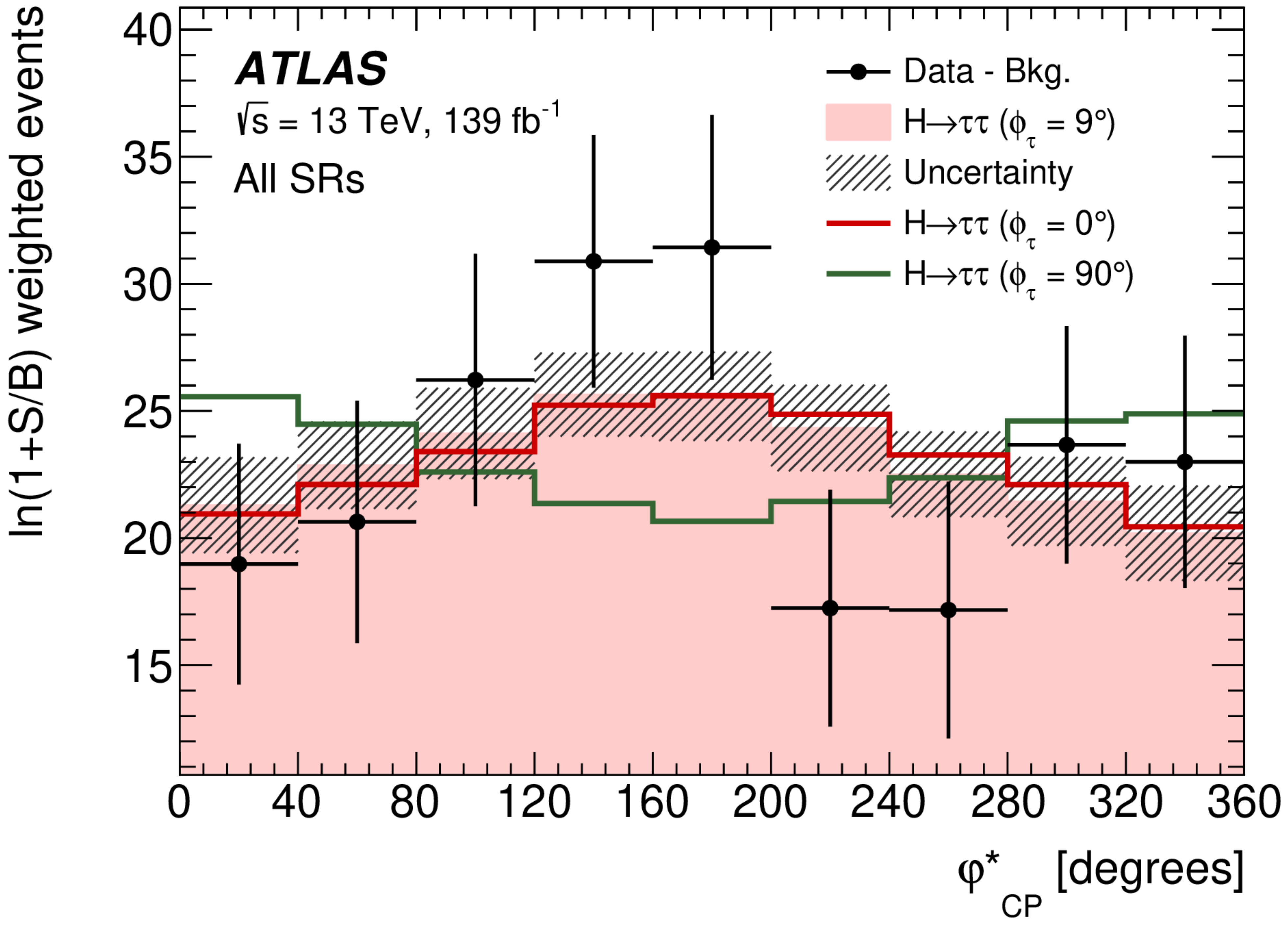

- Simultaneous likelihood fit as a function of the CP mixing angle α (ϕ_τ here).
- Signal strength floating in the fit.
- Best fit value: $\alpha = 9^\circ \pm 16^\circ$
- Reject the pure CP-odd hypothesis at 3.4 σ level.
- Results are consistent with the SM.

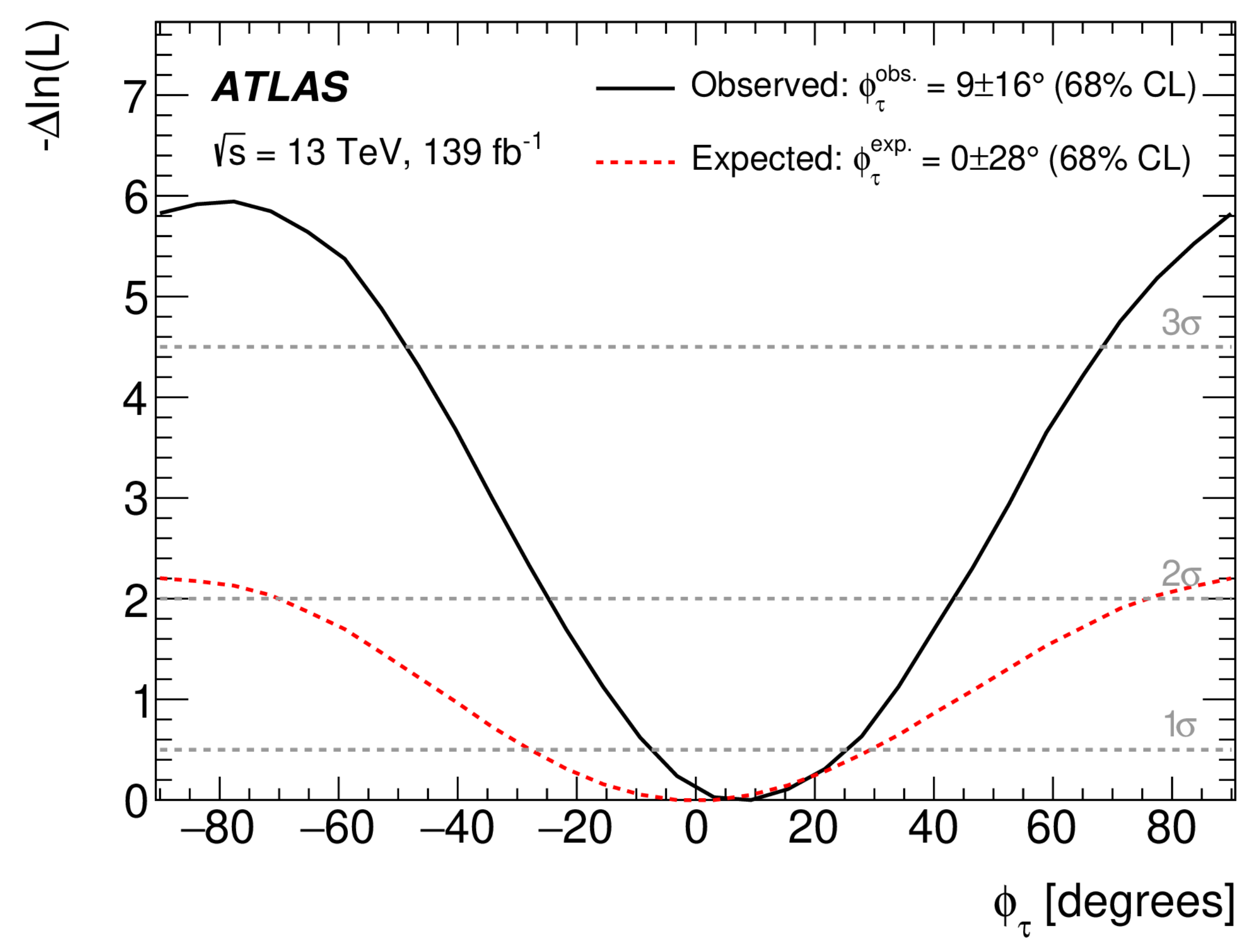

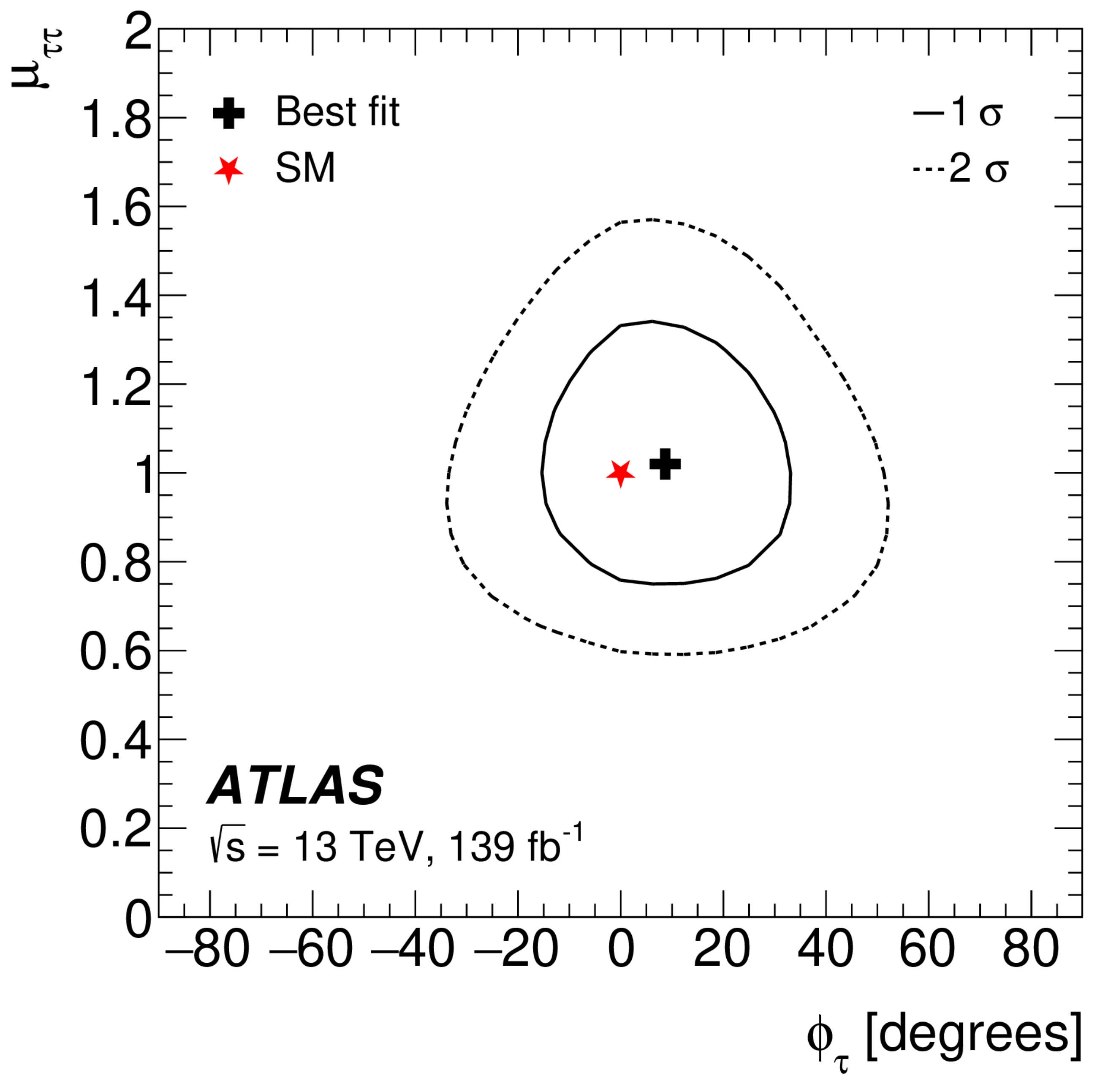

Summary and Outlook

- Four ATLAS-searches for CP violation in the Higgs sector, both in Higgs production and decay, utilising the full Run 2 dataset.
- No evidence for CP violation observed.
- All four analyses use multivariate methods to improve sensitivity.
- Complimentary analyses, such as VBF $H \to \tau\bar{\tau}$ and Ht with $H \to b\bar{b}$ are in the pipeline.
- Searches utilising Run 3 data are also under way.

Backup

Introduction

- Sakharov conditions: CP violation must exist to explain the matter-antimatter asymmetry in the universe.
    - CP violation exists in the SM, but not enough to explain the observed asymmetry.
- In the SM, the Higgs boson is a CP-even scalar ($J^P = 0^+$).
    - Pure CP-odd pseudoscalar ($J^P = 0^-$) state has been ruled out.
    - Mixed states still possible.
- Observation of CP violation in the Higgs sector would be unequivocal evidence of BSM physics.

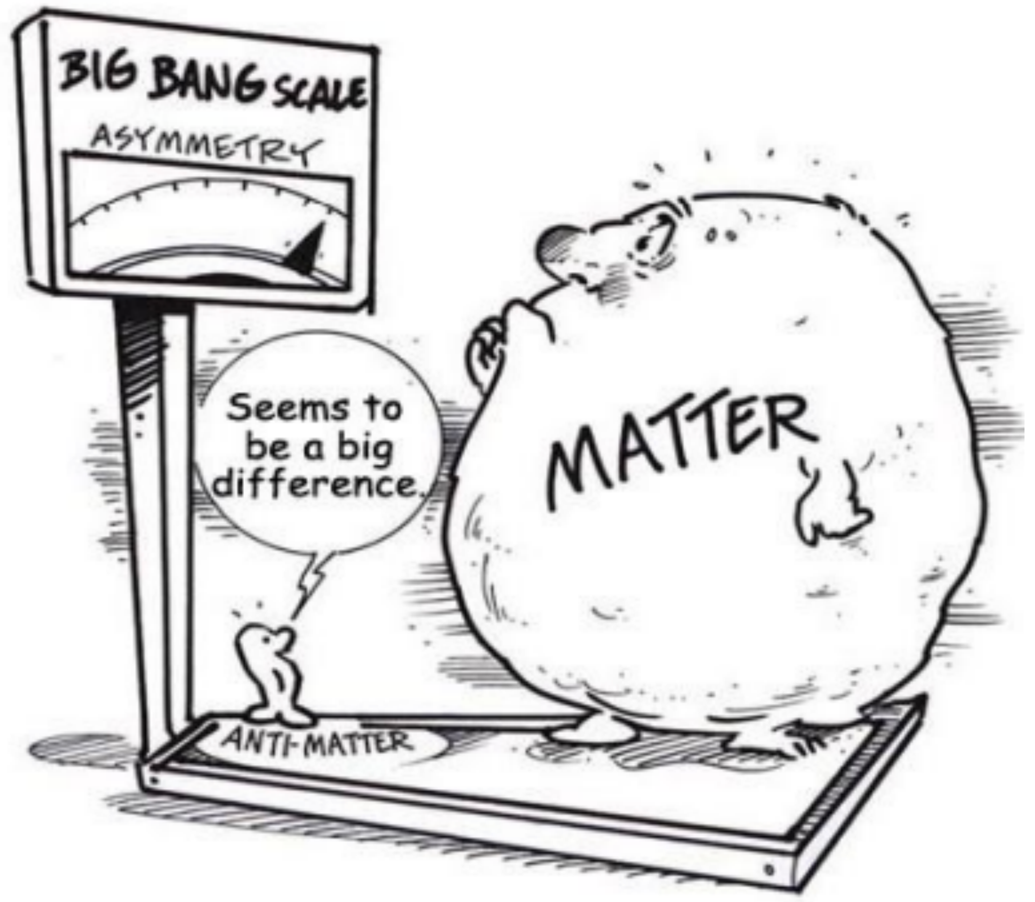

Introduction

- The ATLAS detector recorded 139 fb^{-1} of proton-proton collision data during the 2015-2018 LHC data taking campaign (Run 2).

- This talk will present recent ATLAS searches for CP violation in Higgs production and decay, utilising the full Run 2 dataset.

- Probing both bosonic and fermionic Higgs couplings.

ATLAS Public Luminosity Results

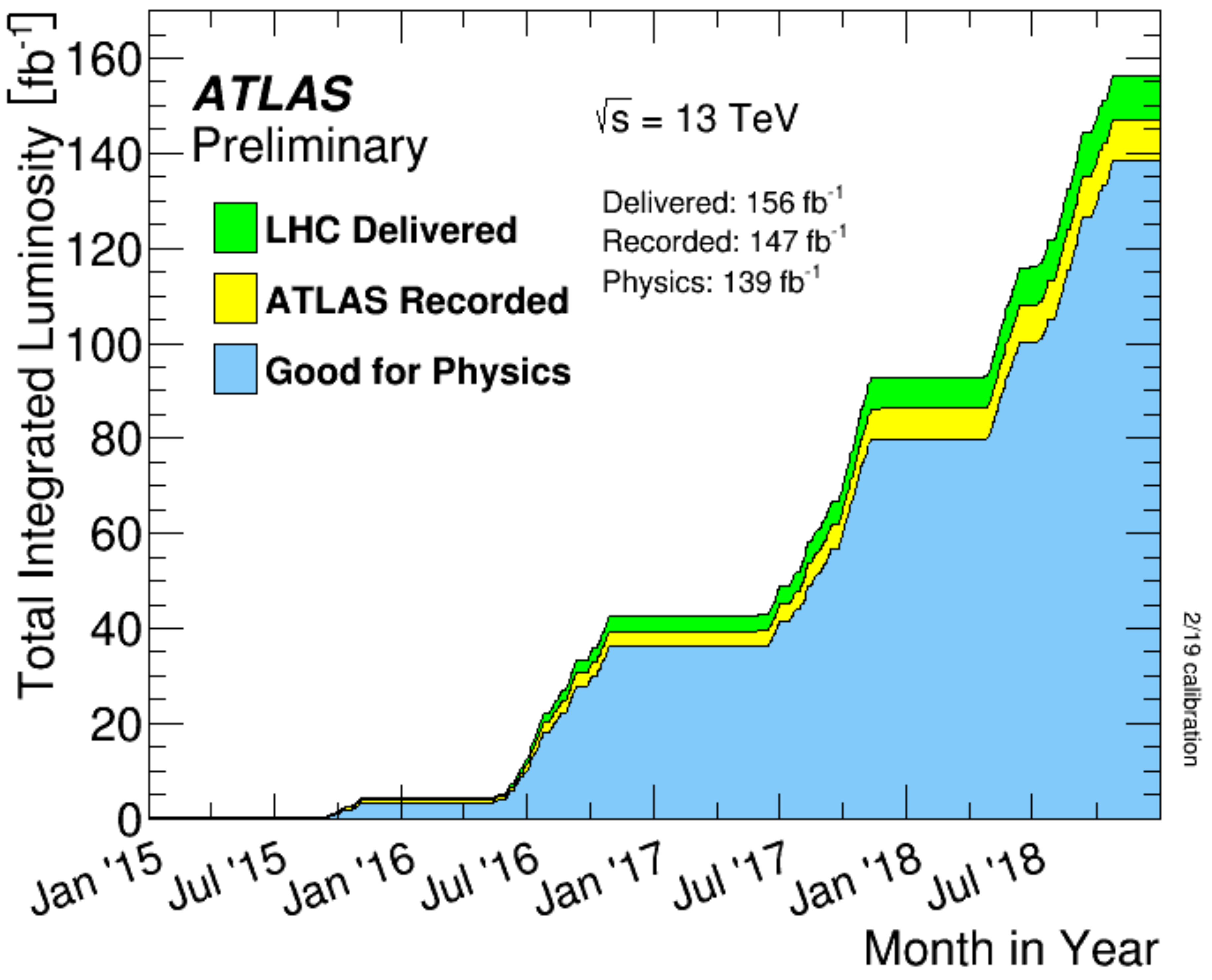

Theoretical Framework - SMEFT

- Extend the SM Lagrangian by CP violating operators of mass dimension 6:

$$\mathscr{L}_{EFT} = \mathscr{L}_{SM} + \sum_i \frac{c_i}{\Lambda^2} \mathcal{O}_i^{(6)}$$

The Warsaw Basis

Operator	Field Content	Wilson Coefficient
$\mathcal{O}_{\Phi\widetilde{W}}$	$\Phi^\dagger\Phi\widetilde{W}^i_{\mu\nu}W^{i\mu\nu}$	$c_{H\widetilde{W}}$
$\mathcal{O}_{\Phi\widetilde{B}}$	$\Phi^\dagger\Phi\widetilde{B}_{\mu\nu}B^{\mu\nu}$	$c_{H\widetilde{B}}$
$\mathcal{O}_{\Phi\widetilde{W}B}$	$\Phi^\dagger\sigma^i\Phi\widetilde{W}^i_{\mu\nu}B^{\mu\nu}$	$c_{H\widetilde{W}B}$

The Higgs Basis

Operator	Field Content	Wilson Coefficient
$\mathcal{O}_{hZ\widetilde{Z}}$	$hZ_{\mu\nu}\widetilde{Z}^{\mu\nu}$	c_{ZZ}
$\mathcal{O}_{hA\widetilde{A}}$	$hA_{\mu\nu}\widetilde{A}^{\mu\nu}$	$c_{\gamma\gamma}$
$\mathcal{O}_{hZ\widetilde{A}}$	$hZ_{\mu\nu}\widetilde{A}^{\mu\nu}$	$c_{Z\gamma}$

The HISZ Basis

- In VBF, we cannot separate the contribution from different boson flavours.
- Set $c_{H\widetilde{W}} = c_{H\widetilde{B}} = \frac{\Lambda^2}{v^2}\tilde{d}$, $c_{H\widetilde{W}B} = 0$
- CP-odd contribution is now parameterised through $\tilde{d}$ alone.

Theoretical Framework - SMEFT

- Cross section is proportional to the squared matrix element:

$$|\mathcal{M}|^2 = |\mathcal{M}_{SM}|^2 + 2\sum_i \frac{c_i}{\Lambda^2} Re(\mathcal{M}^*_{SM}\mathcal{M}_{BSM,i}) + \sum_i \sum_j \frac{c_i c_j}{\Lambda^4} Re(\mathcal{M}^*_{BSM,j}\mathcal{M}_{BSM,i})$$

- The first and third terms are both CP-even.
- The second term, stemming from interference between the SM and BSM matrix elements, is CP-odd.

The Kappa Framework

$$\kappa_t = \kappa_t' \cos\alpha$$
$$\tilde{\kappa}_t = \kappa_t' \sin\alpha$$

- Example: top Yukawa coupling: $\mathscr{L}_{t\bar{t}H} = y_t \phi \bar{\psi}_t \psi_t$
- Add pseudoscalar term: $\mathscr{L}_{t\bar{t}H} = -y_t \phi \bar{\psi}_t (\kappa_t + i\gamma_5 \tilde{\kappa}_t) \psi_t$
- Expressed in terms of mixing angle α: $\mathscr{L}_{t\bar{t}H} = -\kappa_t' y_t \phi \bar{\psi}_t (\cos\alpha + i\gamma_5 \sin\alpha) \psi_t$
- Pure CP-even (α=0), pure CP-odd (α=π/2). Intermediate values are possible.
- CP-odd component of the HVV coupling is naturally suppressed by the scale of the new physics (Λ). This does not happen for Yukawa couplings, where CP-odd contribution may be significant at tree level.

Optimal observable distribution in the four VBF SRs, as well as in the inclusive SR.

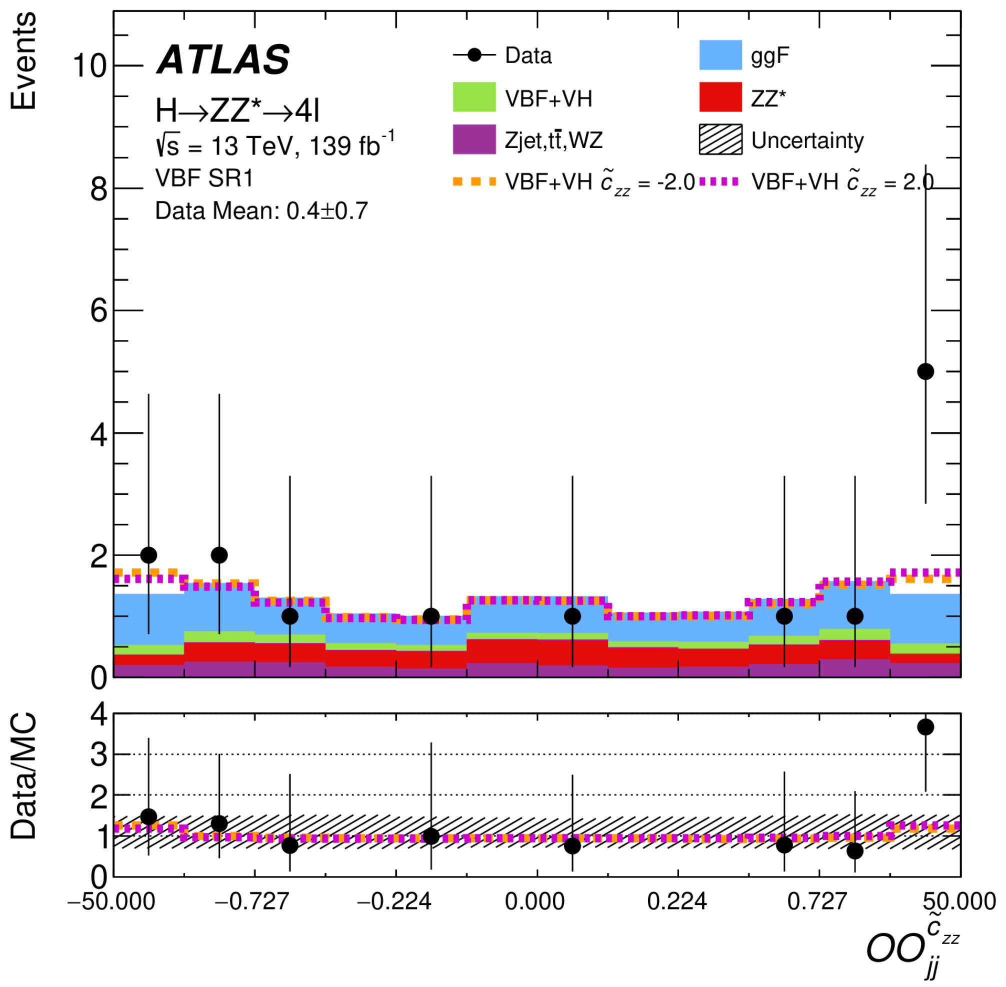

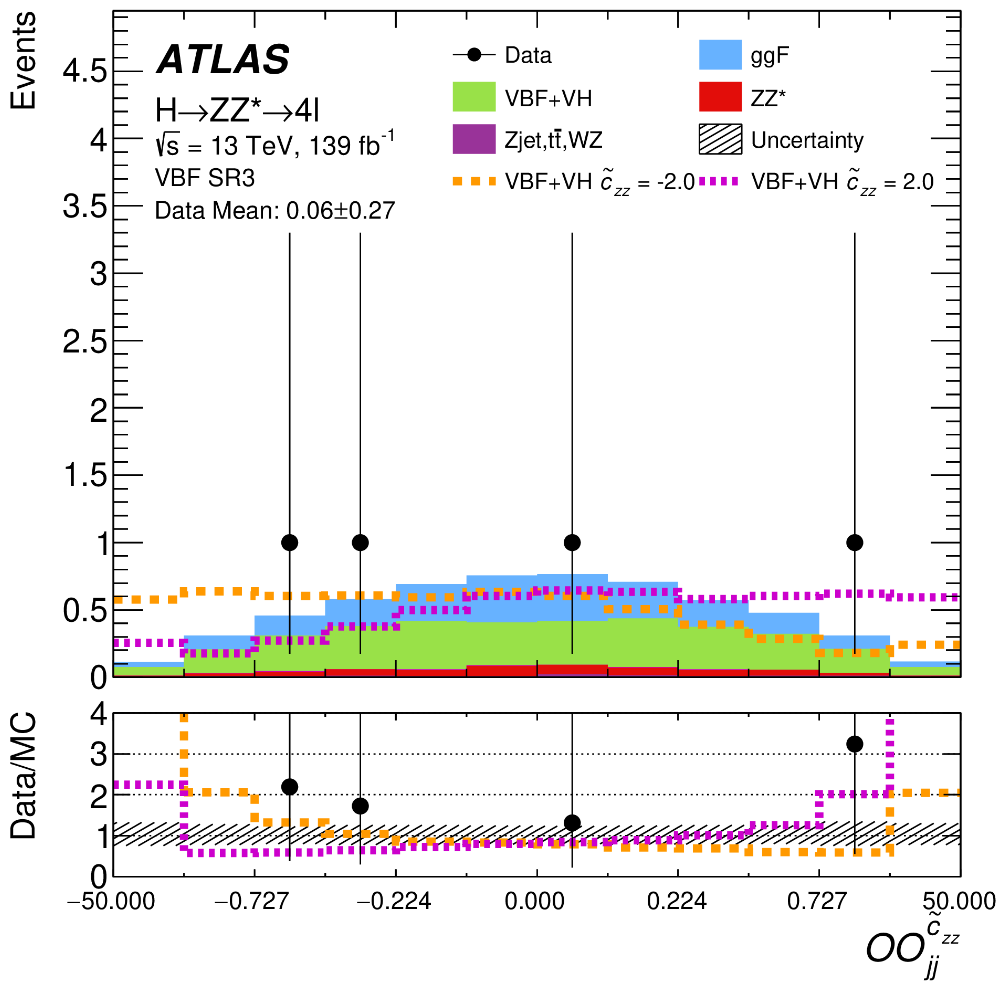

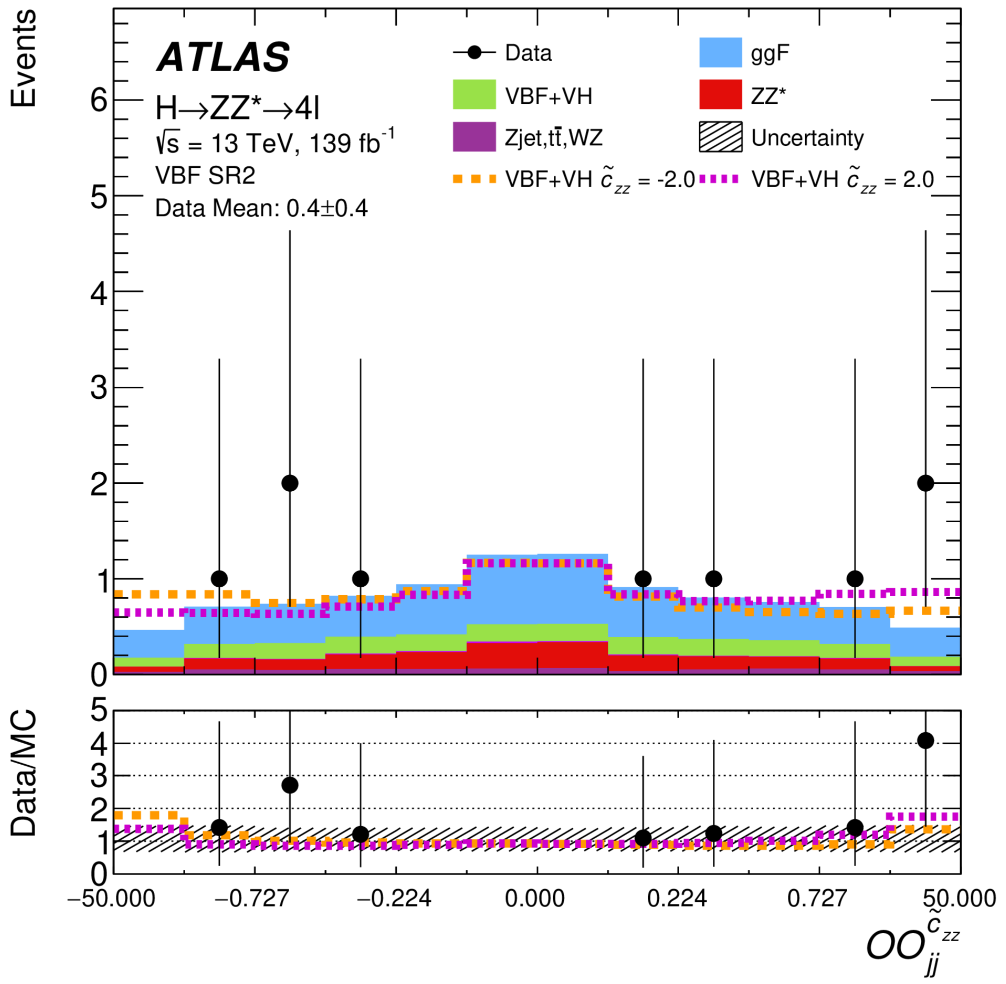

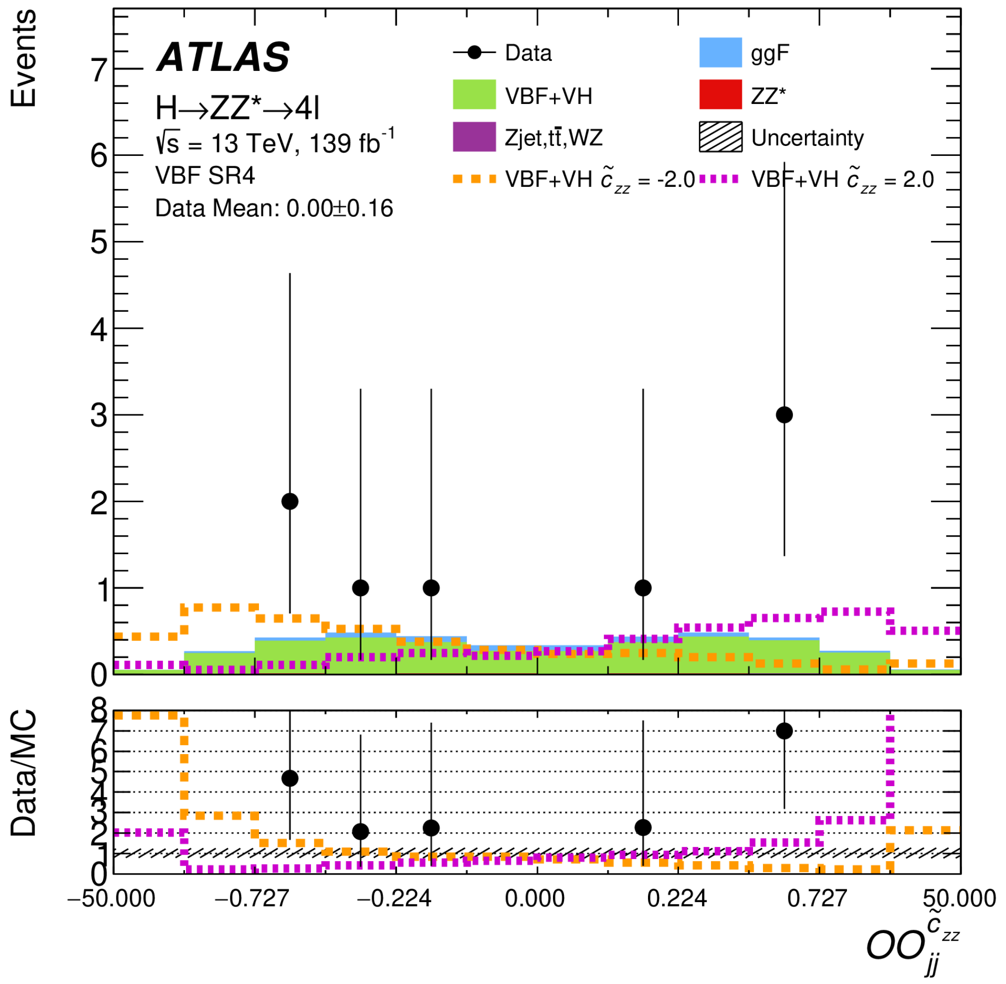

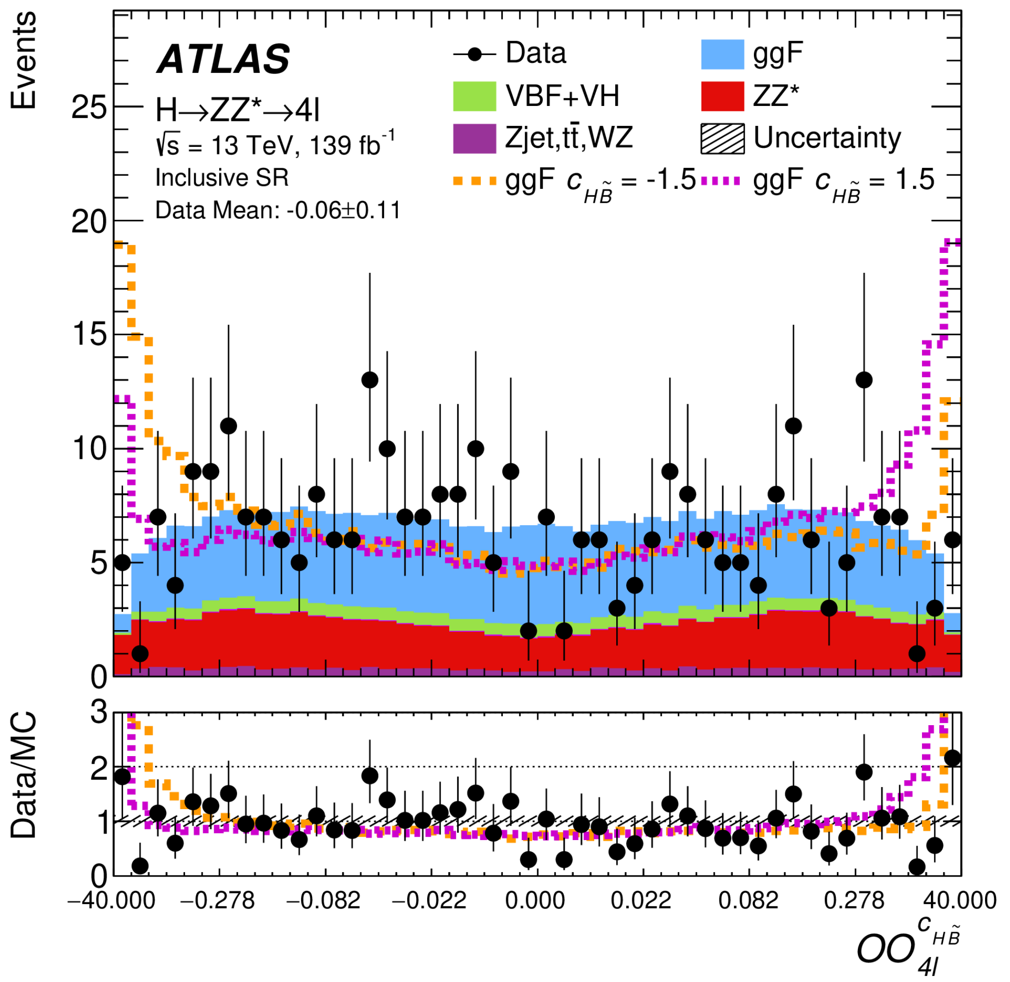

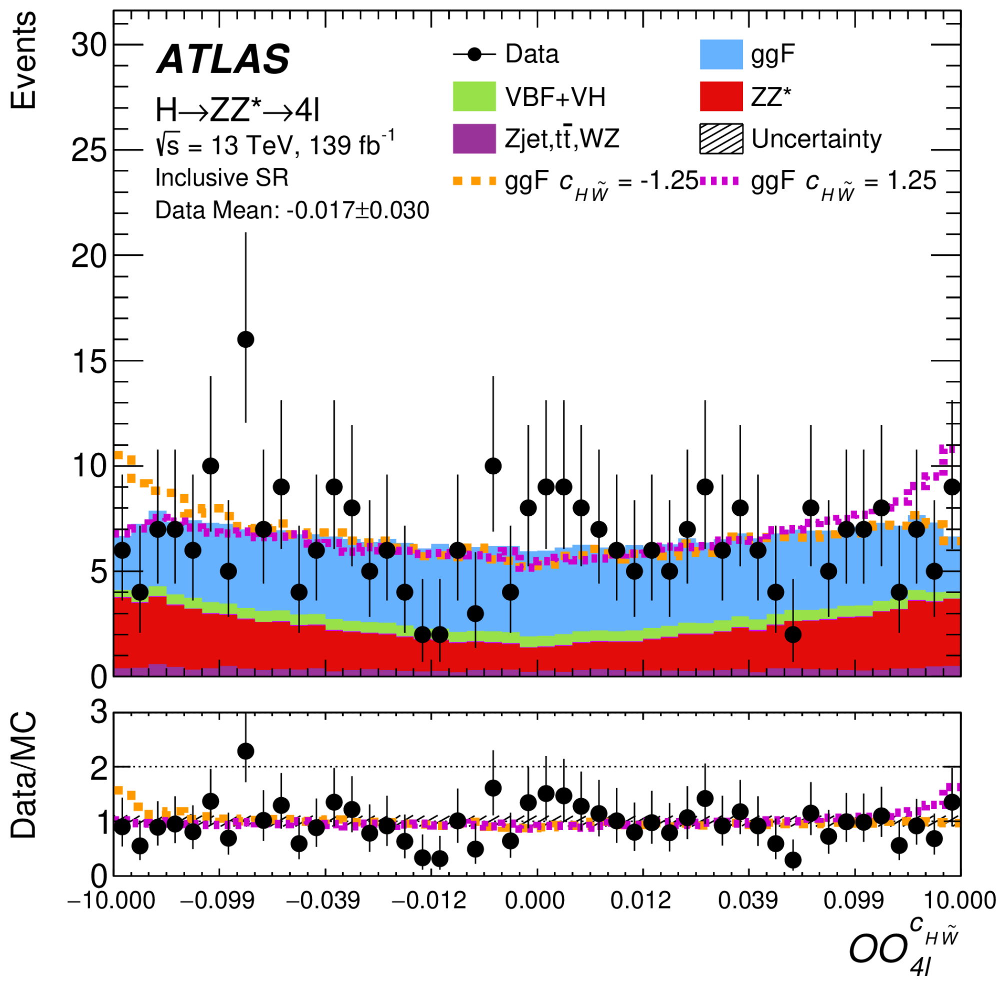

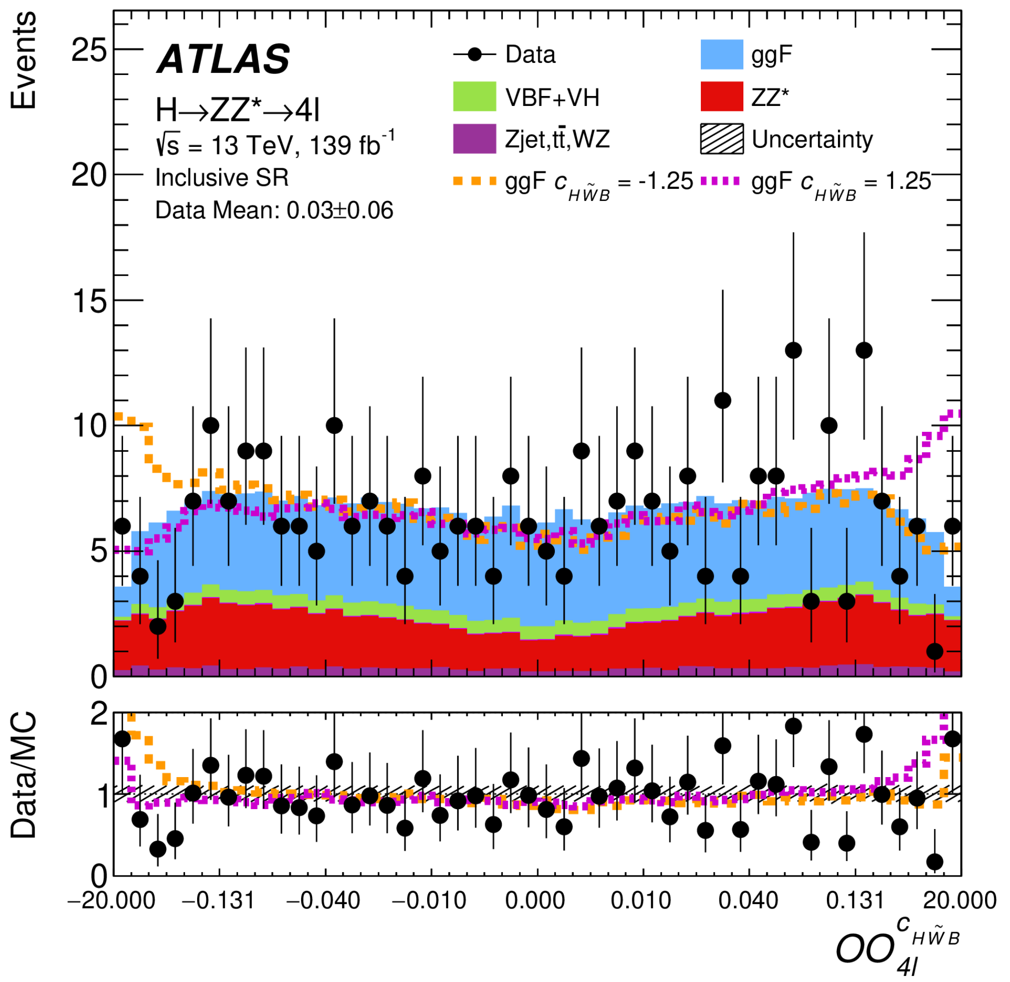

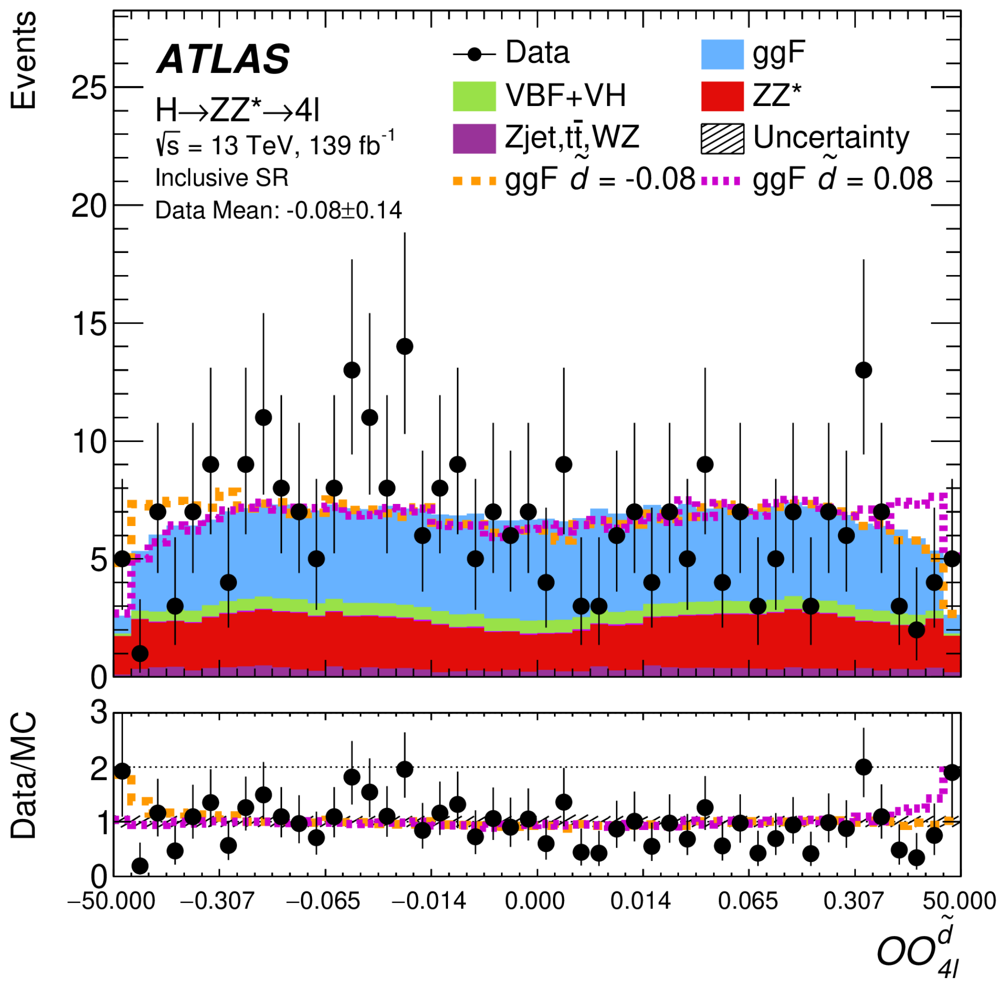

H → ZZ* → 4l

[arXiv:2304.09612 (submitted to JHEP)](https://arxiv.org/abs/2304.09612)

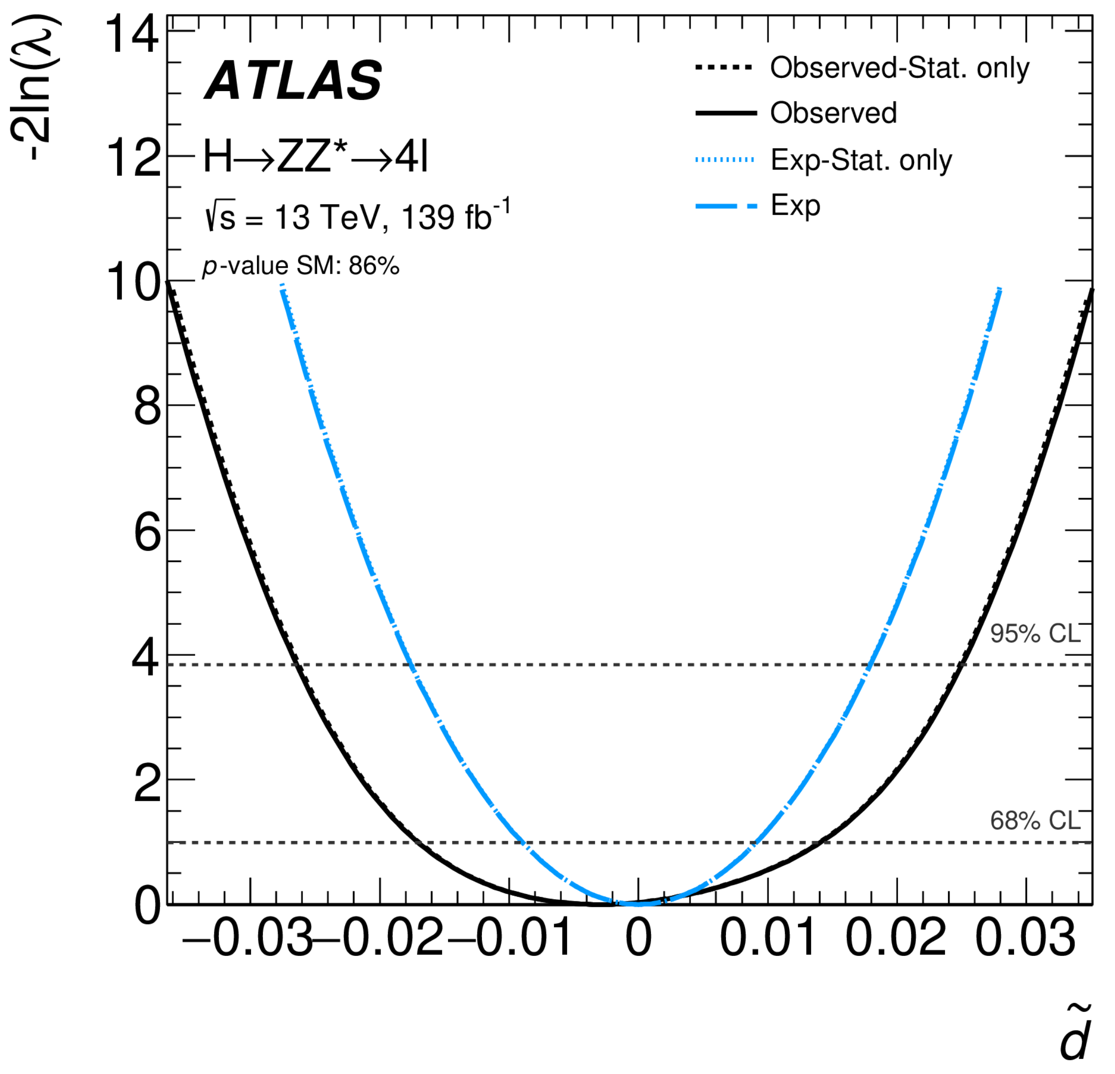

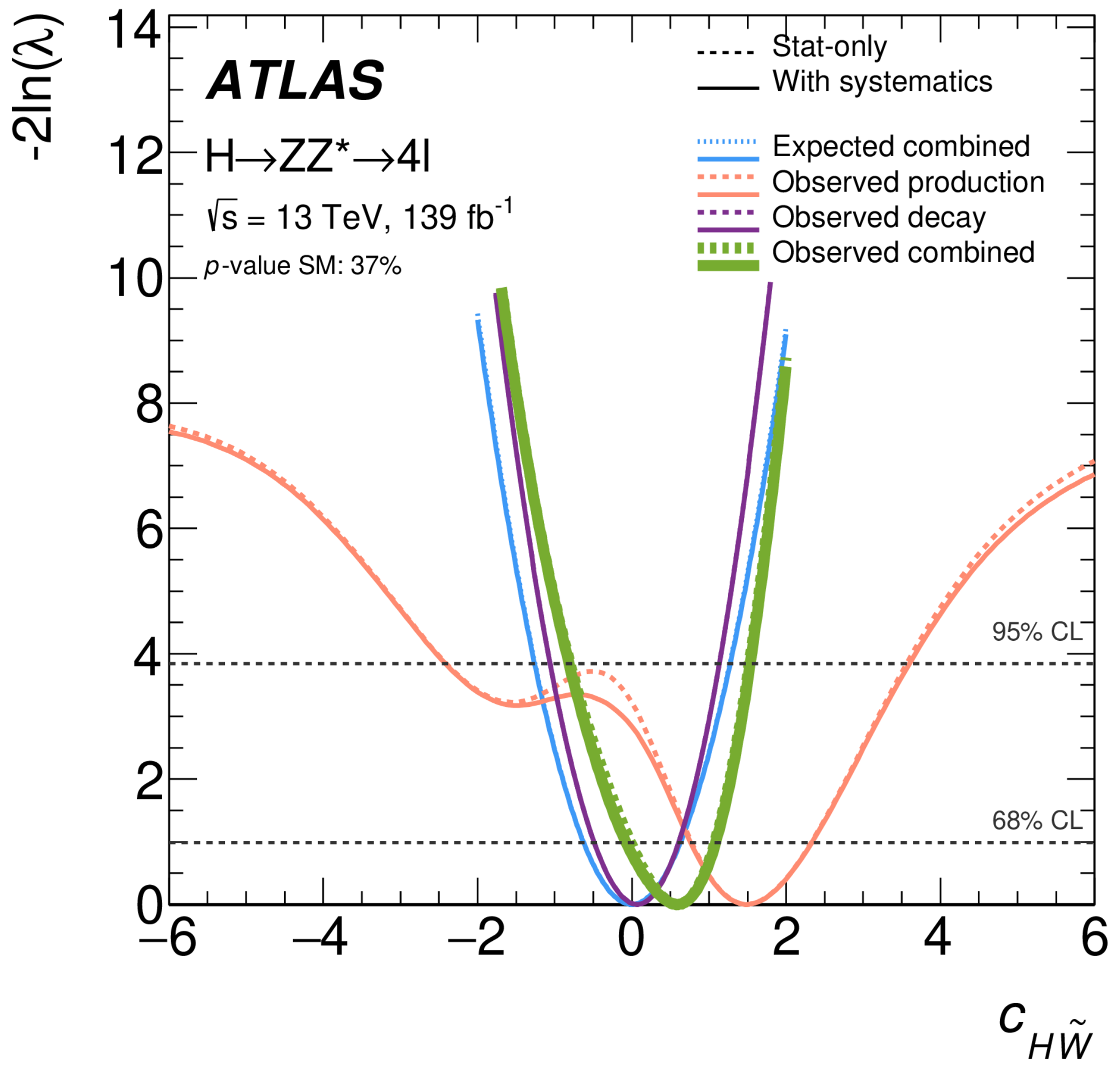

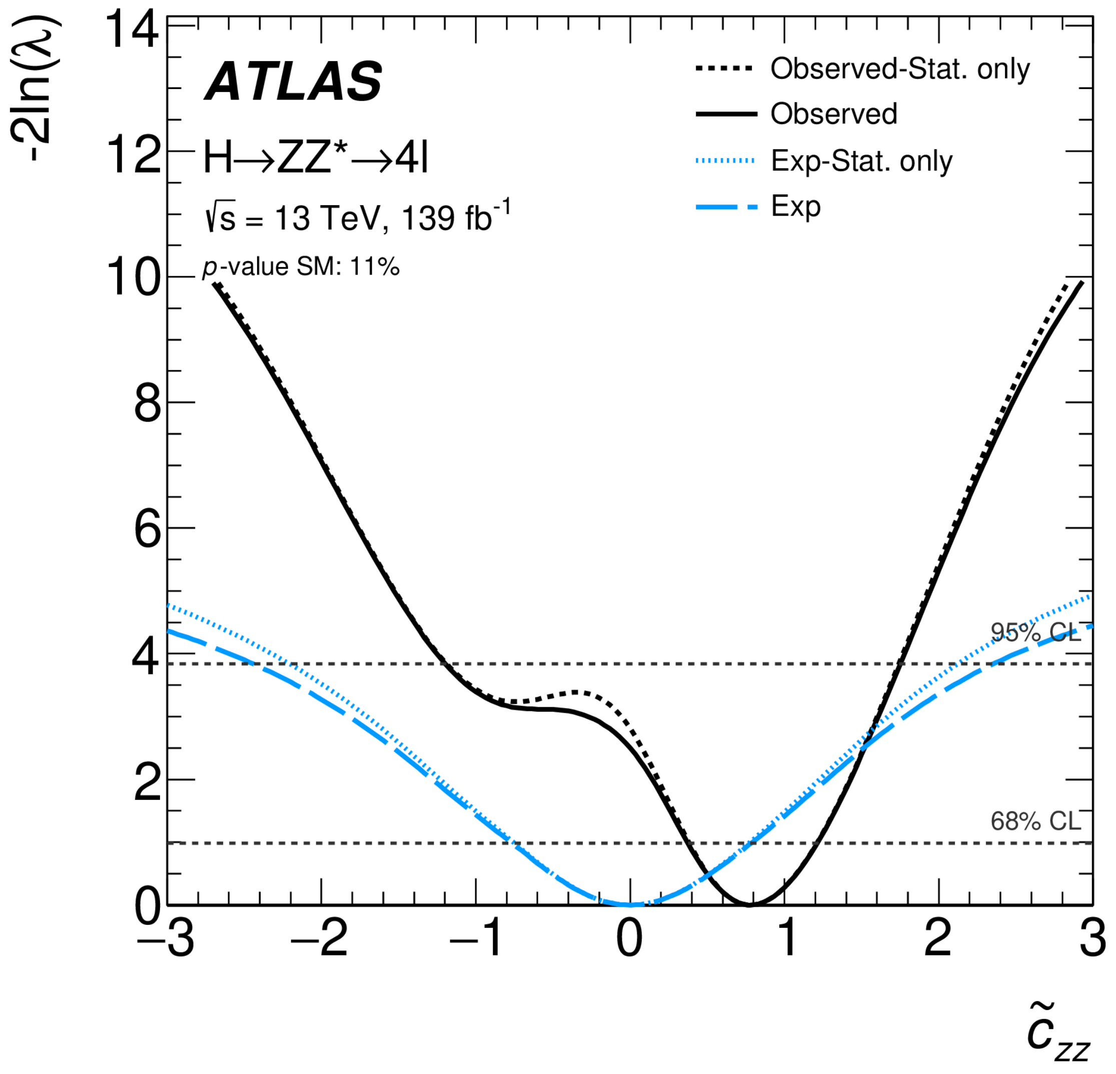

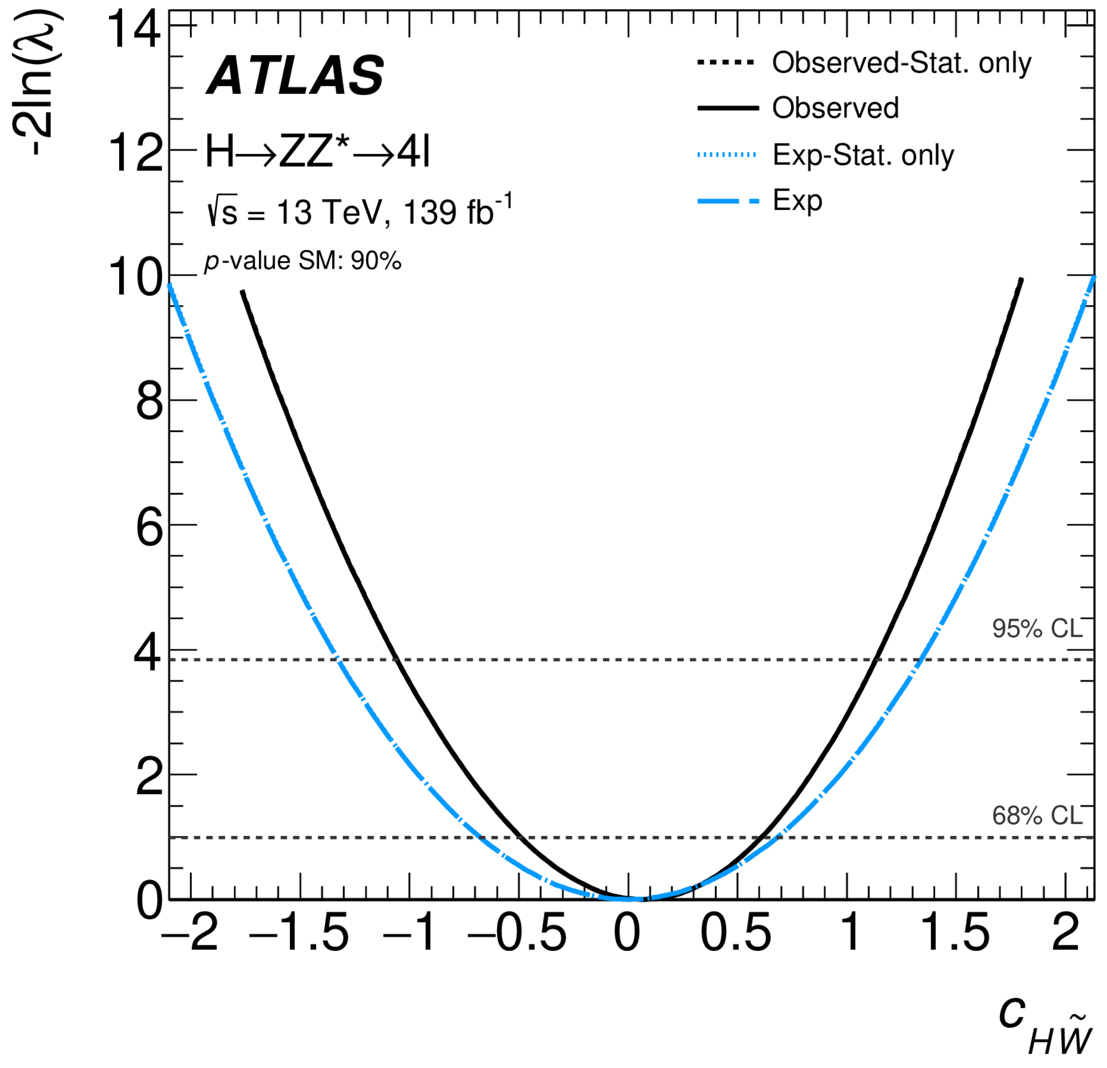

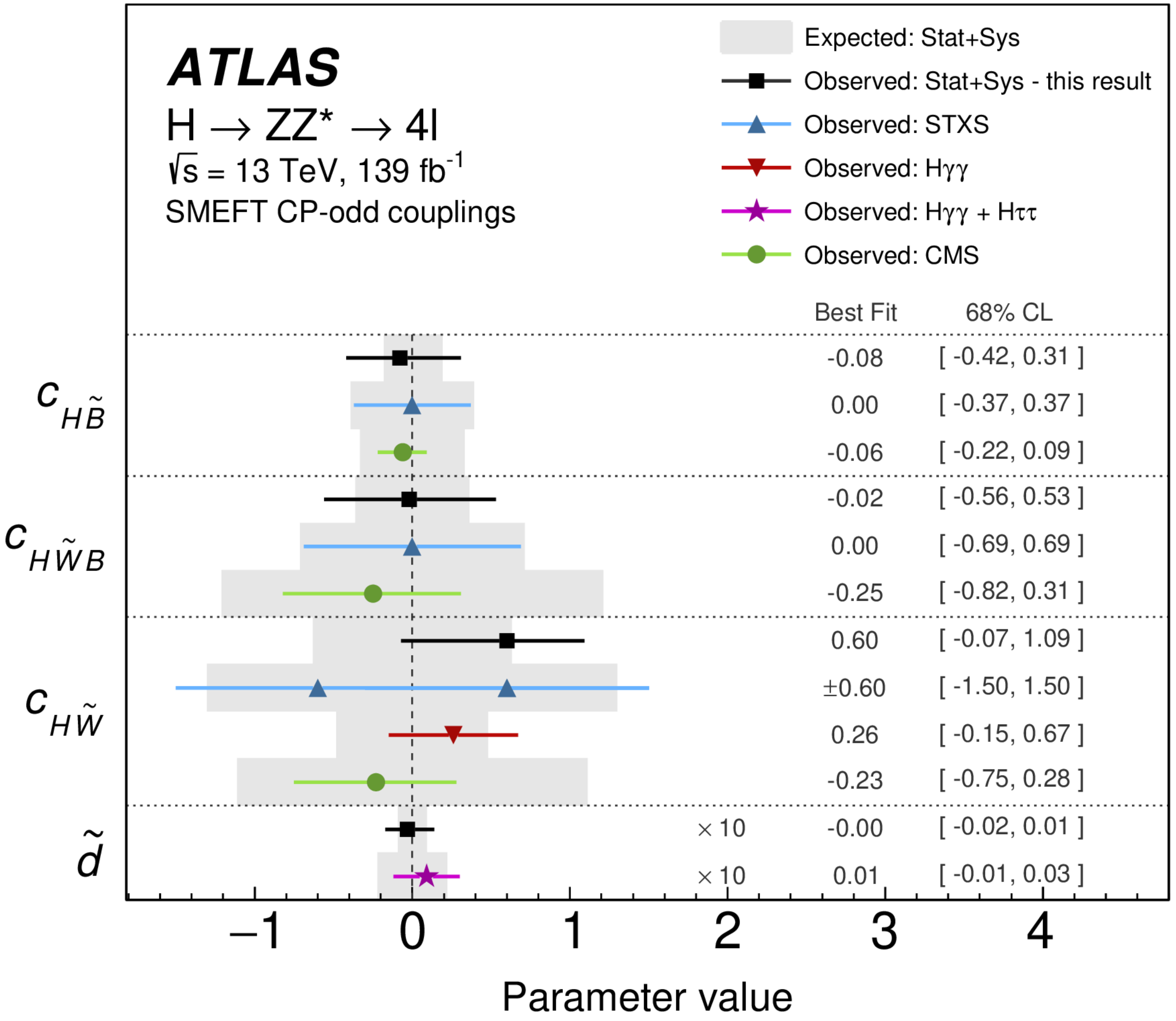

VBF H $\to \gamma\gamma$

Phys. Rev. Lett. 131 (2023) 061802

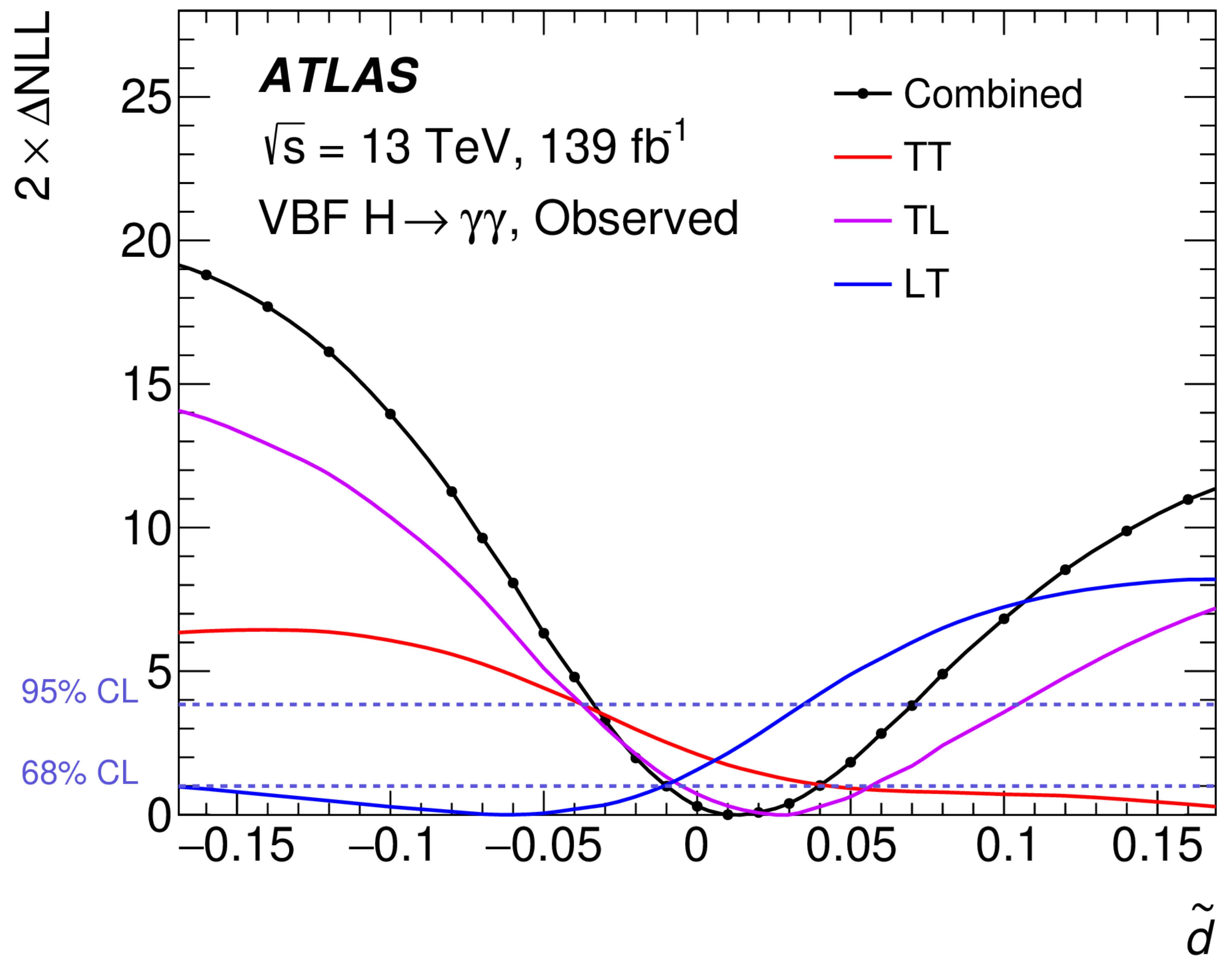

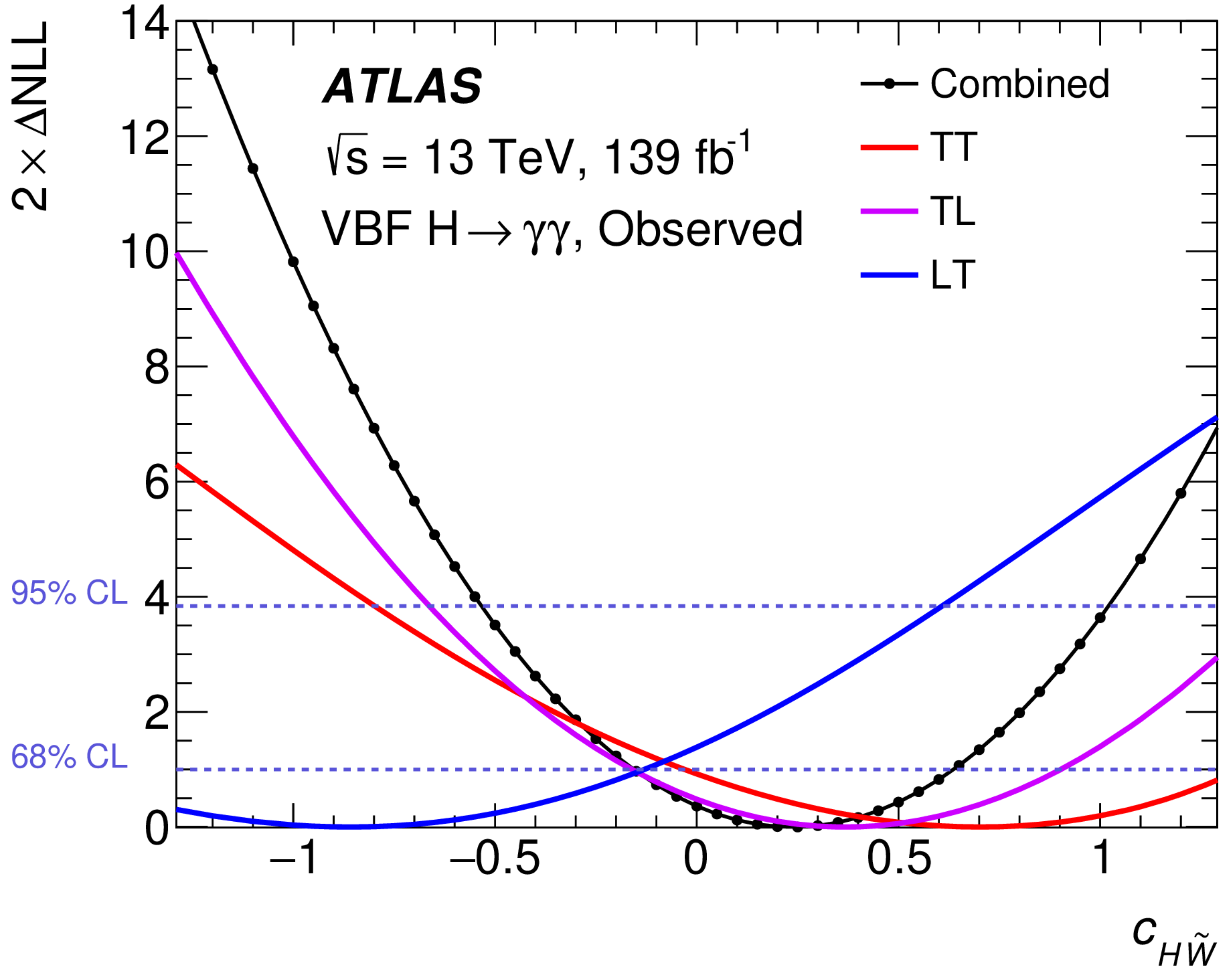

Ht, $Ht\bar{t}$ with $H \to b\bar{b}$

Phys. Lett. B 849 (2024) 138469

Channel (TR)	Final SRs and CRs	Classification BDT selection	Fitted observable
Dilepton ($TR^{\geq 4j, \geq 4b}$)	$CR_{\text{no-reco}}^{\geq 4j, \geq 4b}$	–	$\Delta\eta_{\ell\ell}$
	$CR^{\geq 4j, \geq 4b}$	$BDT^{\geq 4j, \geq 4b} \in [-1, -0.086)$	b_4
	$SR_1^{\geq 4j, \geq 4b}$	$BDT^{\geq 4j, \geq 4b} \in [-0.086, 0.186)$	b_4
	$SR_2^{\geq 4j, \geq 4b}$	$BDT^{\geq 4j, \geq 4b} \in [0.186, 1]$	b_4
ℓ+jets ($TR^{\geq 6j, \geq 4b}$)	$CR_1^{\geq 6j, \geq 4b}$	$BDT^{\geq 6j, \geq 4b} \in [-1, -0.128)$	b_2
	$CR_2^{\geq 6j, \geq 4b}$	$BDT^{\geq 6j, \geq 4b} \in [-0.128, 0.249)$	b_2
	$SR^{\geq 6j, \geq 4b}$	$BDT^{\geq 6j, \geq 4b} \in [0.249, 1]$	b_2
ℓ+jets (TR_{boosted})	SR_{boosted}	$BDT^{\text{boosted}} \in [-0.05, 1]$	BDT^{boosted}

Ht, $Ht\bar{t}$ with $H \to b\bar{b}$

Phys. Lett. B 849 (2024) 138469

- Yields in the l + jets channel.

	$CR^{5j,\geq 4b}_{lo}$	$CR^{5j,\geq 4b}_{hi}$	$CR^{\geq 6j,\geq 4b}_{1}$	$CR^{\geq 6j,\geq 4b}_{2}$	$SR^{\geq 6j,\geq 4b}$	$SR_{boosted}$
$t\bar{t}H$ $(1, 0°)$	60 ± 9	63 ± 10	78 ± 11	139 ± 18	173 ± 26	46 ± 6
$tH(1, 0°)$	3.5 ± 0.5	3.8 ± 0.6	3.3 ± 0.6	2.3 ± 0.6	1.3 ± 0.4	1.9 ± 0.4
$t\bar{t}H$ $(1, 90°)$	28 ± 6	28 ± 6	45 ± 11	61 ± 12	68 ± 16	45 ± 6
$tH(1, 90°)$	19.0 ± 2.8	19.4 ± 3.1	17.4 ± 3.1	13.1 ± 3.5	10 ± 4	29 ± 6
$t\bar{t}H$ $(0.84, 11°)$	40 ± 30	41 ± 31	50 ± 40	90 ± 70	110 ± 80	30 ± 22
tH $(0.84, 11°)$	3 ± 4	3.9 ± 1.9	3.1 ± 1.9	1.9 ± 0.8	1.3 ± 1.7	3 ± 5
$t\bar{t}+\geq 1b$	1530 ± 80	1090 ± 60	4300 ± 120	2220 ± 120	1110 ± 110	335 ± 30
$t\bar{t}+\geq 1c$	650 ± 50	96 ± 11	950 ± 80	450 ± 40	153 ± 15	196 ± 22
$t\bar{t}$+ light	280 ± 40	28 ± 8	230 ± 60	117 ± 26	32 ± 11	76 ± 15
Other	173 ± 30	99 ± 20	320 ± 50	159 ± 21	83 ± 11	60 ± 11
Total	2690 ± 50	1350 ± 40	5870 ± 80	3040 ± 70	1500 ± 50	701 ± 31
Data	2696	1363	5837	3090	1470	699

Ht, $Ht\bar{t}$ with $H \to b\bar{b}$

Phys. Lett. B 849 (2024) 138469

- Yields in the dilepton channel.

	$CR^{3j,3b}_{hi}$	$CR^{\geq 4j,3b}_{lo}$	$CR^{\geq 4j,3b}_{hi}$	$CR^{\geq 4j,\geq 4b}_{no\text{-}reco}$	$CR^{\geq 4j,\geq 4b}$	$SR^{\geq 4j,\geq 4b}_{1}$	$SR^{\geq 4j,\geq 4b}_{2}$
$t\bar{t}H$ (1, 0°)	26 ± 4	79 ± 8	120 ± 12	16.9 ± 2.1	6.9 ± 1.1	12.5 ± 1.5	24.8 ± 2.9
tH(1, 0°)	1.12 ± 0.13	0.90 ± 0.13	1.74 ± 0.20	0.19 ± 0.08	0.087 ± 0.035	0.100 ± 0.033	0.09 ± 0.06
$t\bar{t}H$ (1, 90°)	10.6 ± 1.6	35.6 ± 3.5	54 ± 5	7.2 ± 0.9	4.3 ± 0.6	6.1 ± 0.7	10.9 ± 1.3
tH(1, 90°)	5.4 ± 0.6	7.0 ± 1.0	10.7 ± 1.2	1.8 ± 0.8	0.48 ± 0.19	0.48 ± 0.16	0.5 ± 0.4
$t\bar{t}H$ (0.84, 11°)	18 ± 14	50 ± 40	80 ± 60	11 ± 9	4.7 ± 3.4	8 ± 6	17 ± 12
tH (0.84, 11°)	0.9 ± 0.5	1.0 ± 1.9	1.5 ± 1.3	0.17 ± 0.16	0.068 ± 0.016	0.08 ± 0.14	0.07 ± 0.09
$t\bar{t}+\geq 1b$	1990 ± 80	2520 ± 110	4040 ± 130	288 ± 15	371 ± 16	160 ± 8	122 ± 11
$t\bar{t}+\geq 1c$	550 ± 50	2510 ± 150	1160 ± 90	23 ± 4	31.1 ± 2.5	13.4 ± 1.6	8.2 ± 1.0
$t\bar{t}+$ light	143 ± 27	960 ± 130	230 ± 40	1.7 ± 0.4	2.3 ± 0.8	1.4 ± 0.8	0.57 ± 0.25
Other	140 ± 11	390 ± 19	340 ± 40	33 ± 8	18.6 ± 2.5	10.9 ± 1.3	8.7 ± 1.0
Total	2840 ± 50	6430 ± 80	5850 ± 80	358 ± 12	428 ± 15	194 ± 5	156 ± 6
Data	2827	6429	5865	354	420	190	170

Ht, $Ht\bar{t}$ with $H \rightarrow b\bar{b}$

Phys. Lett. B 849 (2024) 138469

- Sources of uncertainty on α and κ_t'

Uncertainty source	$\Delta\alpha\,[^\circ]$	
Process modelling		
Signal modelling	+8.8	-14
$t\bar{t}+\geq 1b$ modelling		
$t\bar{t}+\geq 1b$ 4V5 FS	+23	-37
$t\bar{t}+\geq 1b$ NLO matching	+22	-33
$t\bar{t}+\geq 1b$ fractions	+14	-21
$t\bar{t}+\geq 1b$ FSR	+5.2	-9.9
$t\bar{t}+\geq 1b$ PS & hadronisation	+16	-24
$t\bar{t}+\geq 1b$ $p_T^{b\bar{b}}$ shape	+5.4	-4.6
$t\bar{t}+\geq 1b$ ISR	+14	-24
$t\bar{t}+\geq 1c$ modelling	+6.6	-11
$t\bar{t}$ + light modelling	+2.5	-4.7
b-tagging efficiency and mis-tag rates		
b-tagging efficiency	+8.7	-15
c-mis-tag rates	+6.7	-11
l-mis-tag rates	+2.3	-2.7
Jet energy scale and resolution		
b-jet energy scale	+1.6	-3.8
Jet energy scale (flavour)	+7.8	-11
Jet energy scale (pileup)	+5.2	-7.9
Jet energy scale (remaining)	+8.1	-13
Jet energy resolution	+5.7	-9.3
Luminosity	$\leq \pm 1$	
Other sources	+4.9	-8
Total systematic uncertainty	+41	-54
$t\bar{t}+\geq 1b$ normalisation	+8.2	-13
κ_t'	+17	-33
Total statistical uncertainty	+32	-49
Total uncertainty	+52	-73

Uncertainty source	$\Delta\kappa_t'$	
Process modelling		
Signal modelling	+0.10	-0.10
$t\bar{t}+\geq 1b$ modelling		
$t\bar{t}+\geq 1b$ 4V5 FS	+0.08	-0.23
$t\bar{t}+\geq 1b$ NLO matching	+0.15	-0.30
$t\bar{t}+\geq 1b$ fractions	+0.09	-0.21
$t\bar{t}+\geq 1b$ FSR	+0.01	-0.02
$t\bar{t}+\geq 1b$ PS & hadronisation	+0.09	-0.20
$t\bar{t}+\geq 1b$ $p_T^{b\bar{b}}$ shape	+0.07	-0.11
$t\bar{t}+\geq 1b$ ISR	+0.07	-0.17
$t\bar{t}+\geq 1c$ modelling	+0.04	-0.10
$t\bar{t}$ + light modelling	+0.00	-0.01
b-tagging efficiency and mis-tag rates		
b-tagging efficiency	+0.06	-0.12
c-mis-tag rates	+0.03	-0.07
l-mis-tag rates	+0.01	-0.03
Jet energy scale and resolution		
b-jet energy scale	+0.02	-0.02
Jet energy scale (flavour)	+0.01	-0.05
Jet energy scale (pileup)	+0.02	-0.05
Jet energy scale (remaining)	+0.04	-0.08
Jet energy resolution	+0.03	-0.09
Luminosity	$\leq \pm 0.01$	
Other sources	+0.03	-0.07
Total systematic uncertainty	+0.29	-0.45
$t\bar{t}+\geq 1b$ normalisation	+0.05	-0.15
α	+0.08	-0.07
Total statistical uncertainty	+0.09	-0.10
Total uncertainty	+0.30	-0.46

- Acoplanarity distribution in the "high" sensitivity signal regions.

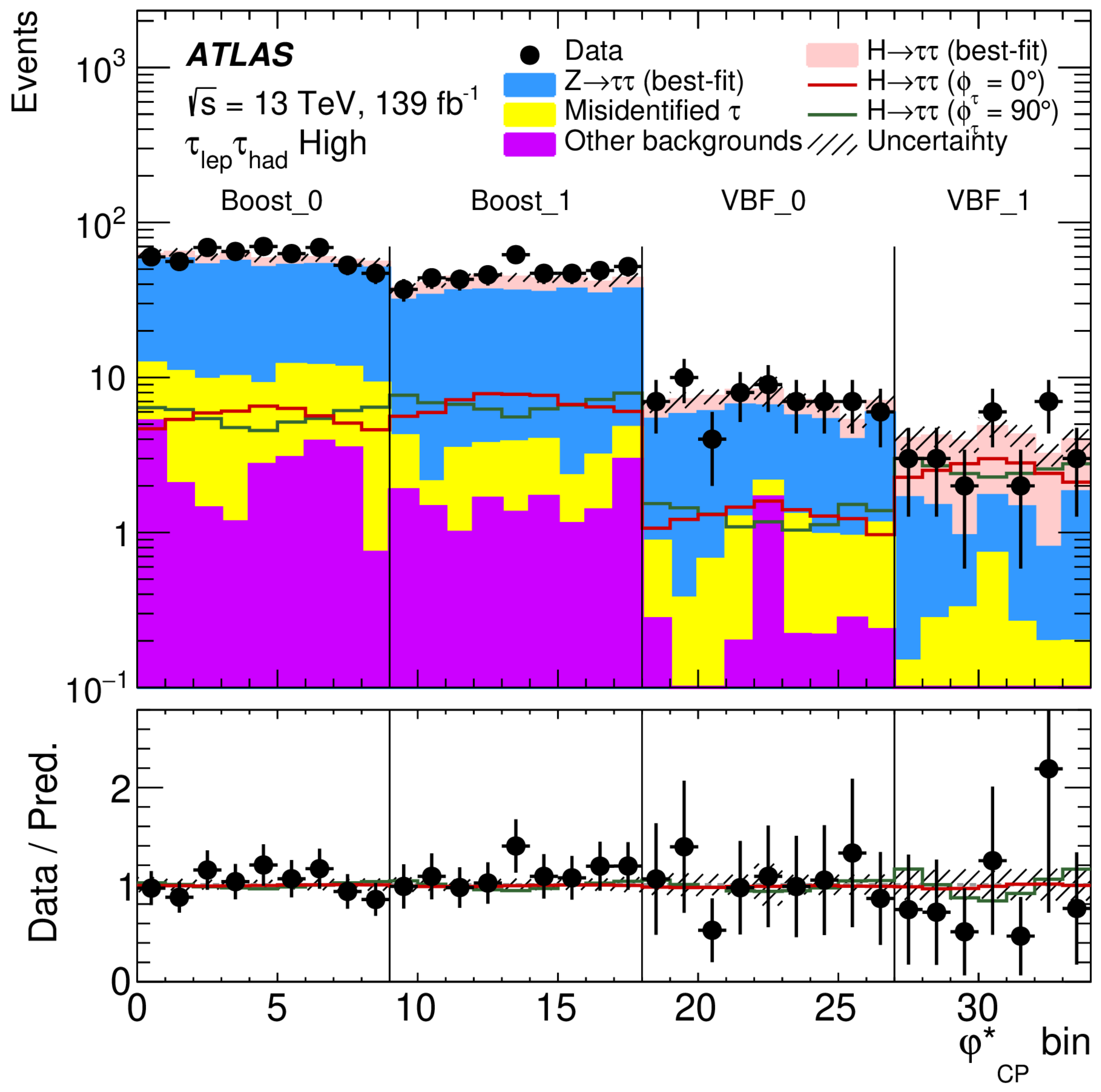

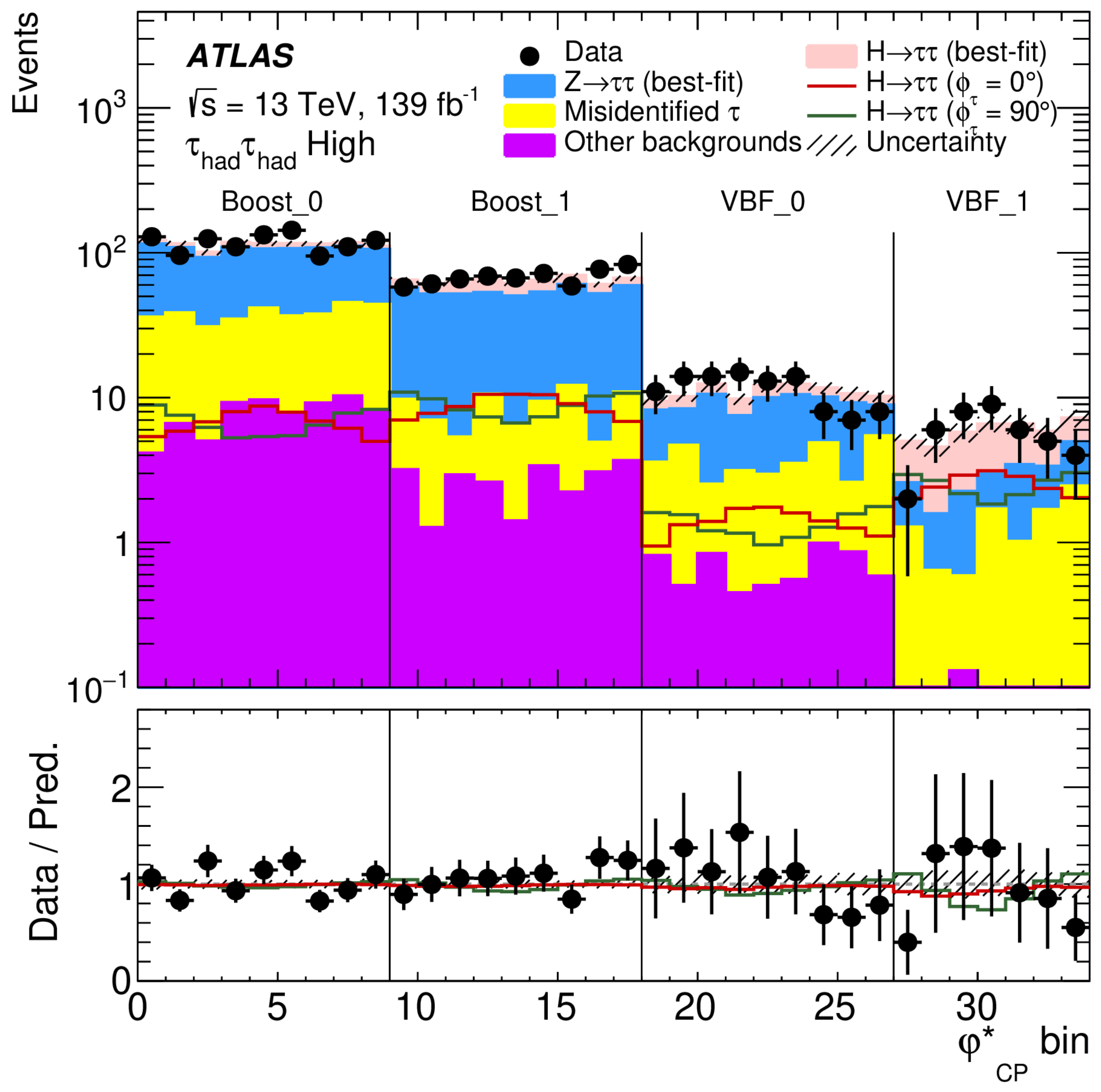

H $\rightarrow \tau\bar{\tau}$

- Branching fractions and selection criteria.

Decay channel	Decay mode combination	Method	Fraction in all τ-lepton-pair decays
$\tau_{lep}\tau_{had}$	ℓ–1p0n	IP	8.1%
	ℓ–1p1n	IP–ρ	18.3%
	ℓ–1pXn	IP–ρ	7.6%
	ℓ–3p0n	IP–a_1	6.9%
$\tau_{had}\tau_{had}$	1p0n–1p0n	IP	1.3%
	1p0n–1p1n	IP–ρ	6.0%
	1p1n–1p1n	ρ	6.7%
	1p0n–1pXn	IP–ρ	2.5%
	1p1n–1pXn	ρ	5.6%
	1p1n–3p0n	ρ–a_1	5.1%

Channel	Signal region	Decay mode combination	Selection criteria
$\tau_{lep}\tau_{had}$	High	ℓ–1p0n	$\lvert d_0^{sig}(e)\rvert > 2.5$ or $\lvert d_0^{sig}(\mu)\rvert > 2.0$ $\lvert d_0^{sig}(\tau_{1p0n})\rvert > 1.5$
		ℓ–1p1n	$\lvert d_0^{sig}(e)\rvert > 2.5$ or $\lvert d_0^{sig}(\mu)\rvert > 2.0$ $\lvert y^{\rho}(\tau_{1p1n})\rvert > 0.1$
	Medium	ℓ–1pXn	$\lvert d_0^{sig}(e)\rvert > 2.5$ or $\lvert d_0^{sig}(\mu)\rvert > 2.0$ $\lvert y^{\rho}(\tau_{1pXn})\rvert > 0.1$
		ℓ–3p0n	$\lvert d_0^{sig}(e)\rvert > 2.5$ or $\lvert d_0^{sig}(\mu)\rvert > 2.0$ $\lvert y^{a_1}(\tau_{3p0n})\rvert > 0.6$
	Low	All above	Not satisfying selection criteria

Channel	Signal region	Decay mode combination	Selection criteria
$\tau_{had}\tau_{had}$	High	1p0n–1p0n	$\lvert d_0^{sig}(\tau_1)\rvert > 1.5$ $\lvert d_0^{sig}(\tau_2)\rvert > 1.5$
		1p0n–1p1n	$\lvert d_0^{sig}(\tau_{1p0n})\rvert > 1.5$ $\lvert y^{\rho}(\tau_{1p1n})\rvert > 0.1$
		1p1n–1p1n	$\lvert y^{\rho}(\tau_1)y^{\rho}(\tau_2)\rvert > 0.2$
	Medium	1p0n–1pXn	$\lvert d_0^{sig}(\tau_{1p0n})\rvert > 1.5$ $\lvert y^{\rho}(\tau_{1pXn})\rvert > 0.1$
		1p1n–1pXn	$\lvert y^{\rho}(\tau_{1p1n})y^{\rho}(\tau_{1pXn})\rvert > 0.2$
		1p1n–3p0n	$\lvert y^{\rho}(\tau_{1p1n})\rvert > 0.1$ $\lvert y^{a_1}(\tau_{3p0n})\rvert > 0.6$
	Low	All above	Not satisfying selection criteria

H $\rightarrow \tau\bar{\tau}$

- Sources of uncertainty on α

Set of nuisance parameters	Impact on ϕ_τ [degrees]
Jet energy scale	3.4
Jet energy resolution	2.5
Pile-up jet tagging	0.5
Jet flavour tagging	0.2
E_T^{miss}	0.4
Electron	0.3
Muon	0.9
τ_{had} reconstruction	1.0
Misidentified τ	0.6
τ_{had} decay mode classification	0.3
π^0 angular resolution and energy scale	0.2
Track ($\pi^\pm$, impact parameter)	0.7
Luminosity	0.1
Theory uncertainty in $H \rightarrow \tau\tau$ processes	1.5
Theory uncertainty in $Z \rightarrow \tau\tau$ processes	1.1
Simulated background sample statistics	1.4
Signal normalisation	1.4
Background normalisation	0.6
Total systematic uncertainty	5.2
Data sample statistics	15.6
Total	16.4